REVISION STATUS SHEET

Document Title: Control Building and Reactor/Fuel Building Complex Seismic Structure-Soil-Structure Interaction Analysis Report

Revision #: 0 **Type:** Engineering Report – Design

Safety Related Classification Code: N/A **MPL No.:** A25-5100, U71-5100, U73-5100, U97-5100

"|" Vertical Sidebar Denotes Change

Rev #	DOORS BL	Change Number	MM/DD/YYYY	Preparing Organization	Issue / Release Status	Verification Status
0	N/A	ECO-0015277	07/15/2015	GEH	Issued for Use-Design	Verified

MADE BY	APPROVALS	AUTH. DATE
Luben Todorovski GEH	Tanya B. Kirby GEH	07/15/2015

REVISION CHART (CONT)

Rev #	DOORS BL	Change Number	MM/DD/YYYY	Preparing Organization	Issue / Release Status	Verification Status

RECORD OF REVISION

Rev #	Description
0	Issue for Use

TABLE OF CONTENTS

LIST OF TABLES

LIST OF FIGURES

LIST OF ACRONYMS

ARS	Acceleration Response Spectra
BE	Best Estimate
CB	Control Building
CPSD	Cumulative Power Spectral Density
DCD	Design Control Document
ESBWR	Economic Simplified Boiling Water Reactor
EW	East-West
FE	Fully Embedded
FFT	Fast Fourier Transformation
FIRS	Foundation Input Response Spectra
ISRS	In-Structure Response Spectra
LB	Lower Bound
LMSM	Lumped Mass-Stick Model
MSM	Modified Subtraction Method
NA3	North Anna Unit 3
NS	North-South
OBE	Operating Basis Earthquake
PE	Partially Embedded
PSD	Power Spectral Density
RB/FB	Reactor Building/Fuel Building
SDOF	Single Degree of Freedom
SRP	Standard Review Plan
SRSS	Square Root of the Sum of the Squares
SSI	Soil-Structure Interaction
SSSI	Structure-Soil-Structure Interaction
UB	Upper Bound

1. INTRODUCTION AND PURPOSE

This report presents the North Anna Unit 3 (NA3) site-specific evaluations of the effects of structure-soil-structure interaction (SSSI) of the large and heavy ESBWR Reactor Building/Fuel Building Complex (RB/FB) on the seismic response of the adjacent small and light Control Building (CB). In the ESBWR standard design control document (DCD), Reference 2-d, an approximate approach was used to evaluate these SSSI effects that considered only the effect of the large and heavy RB/FB on the seismic ground motion at the CB location. A two-steps approach was used in which the ground surface motion at the CB location was first determined from the SSI analysis of the RB/FB standalone model. The calculated ground surface motion at the CB location was then used as input motion to the SSI analysis of the CB standalone model to obtain the seismic response of the CB that included the effects of the RB/FB on the ground motion. The standard design approach to evaluate the SSSI effects of RB/FB on the CB cannot be directly implemented for the NA3 site-specific evaluations because the SSI analyses of RB/FB and CB standalone models use different subgrade profiles representing the subgrade conditions in the vicinity of the two buildings. Therefore, in order to address the effect of subgrade properties variations across the NA3 site, the site-specific SSSI evaluations presented in this report are based on the results of site-specific SSSI analyses using the CB-RB/FB combined model that also provides an explicit representation of the NA3 site conditions between the two buildings and captures the effects of dynamic coupling between the RB/FB and CB at NA3 site.

These site-specific SSSI analyses are performed using the SASSI2010 computer program. The Modified Subtraction Method (MSM) is used in the analyses. The combined SSSI models are developed from the standard design SASSI structural models with full stiffness and Operating Basis Earthquake (OBE) damping described in Section 4.3, coupled with site-specific strain compatible dynamic subsurface properties. The combined models representing the dynamic properties of the CB and RB/FB structures also include the Access Tunnel, that is structurally isolated from the RB/FB and CB, and the near-field subgrade elements providing explicit representation of the subgrade conditions existing between the RB/FB and the CB. The Access Tunnel is modeled using shell elements. The near-field solid elements model the concrete fill and structural fill backfilled below the Access Tunnel and surrounding the CB. The concrete fill is backfilled around and below the building to replace the excavated Zone III rock up to the top of the Zone III rock elevation, and the structural fill is backfilled above the Zone III rock elevation up to the finished ground level grade.

The site-specific SSSI effects of the RB/FB on the CB seismic response are evaluated using the results of the SSSI analyses of the CB-RB/FB combined model for the full column and partial column subgrade profiles representing strain-compatible dynamic soil/rock properties at the CB location. To account for the effects of the potential variability in the properties of the soil and rock, these SSSI evaluations consider two different embedment conditions and two bounding sets of subgrade strain-compatible dynamic properties. The CB-RB/FB SSSI analyses are performed using the CB upper bound (UB) full column, lower bound (LB) and UB partial column profiles and corresponding in-layer input motions applied at the bottom of

the CB foundation. The full column UB and partial column LB subgrade profiles represent the two bounding subgrade stiffness conditions. The UB partial column profile is considered because based on the results in Reference 2-k, it was determined that this case governs the overall seismic response of the CB standalone model.

The in-layer motions are consistent with the envelope of CB Foundation Input Response Spectra (FIRS) and minimum earthquake requirements as specified in Reference 2-h. Section 3 describes the subgrade dynamic properties and input motions used for the CB-RB/FB SSSI analysis that are identical to those used for the SSI analysis of the CB standalone model. The use of identical inputs enables the SSSI effect of the RB/FB on the CB seismic response to be directly evaluated by comparing the results obtained from the SSSI analyses of the CB-RB/FB combined model with the results of the SSI analyses of the CB standalone model.

The site-specific SSSI effects of the RB/FB on the CB site-specific seismic design basis are evaluated by comparing the site-specific CB-RB/FB SSSI analysis results with the corresponding CB site-specific seismic structural loads and In-Structure Response Spectra (ISRS) that are developed as the envelope of the results of the SSI analyses of the CB standalone models with full structural stiffness (uncracked concrete stiffness) and OBE damping. Comparisons are also made with the corresponding seismic loads and ISRS used for the standard design of the CB that are documented in Reference 2-d. Appendix B of Reference 2-k provides a confirmation study that demonstrates the results of the site-specific sensitivity analyses to ensure that the site-specific design basis that is based on the analyses of models with full (uncracked concrete) stiffness properties adequately addresses the effects of structural stiffness variations due to concrete cracking. Therefore, full (uncracked concrete) stiffness is considered for CB-RB/FB SSSI analyses in this report.

1.1 Limitations on Use

This report is issued without limitation.

2. REFERENCES

a. TODI WG3-A25-TDI-S-0004, “North Anna 3 RB/FB, CB & FWSC SSI Analyses EPRI 2013 GMPE Based Inputs”, Revision 0
b. TODI WG3-A25-TDI-S-0006, “North Anna 3 RB/FB, CB & FWSC Outcrop SSI Design Motion Time-Histories”, Revision 0
c. 26A6642AL, “ESBWR Design Control Document Tier 2 Chapter 3 Appendices 3A – 3F”, Revision 10
d. 26A6648, “ESBWR Seismic Analysis of Control Building”, Revision 4
e. WG3-U71-ERD-S-0001, “Reactor/Fuel Building Complex Seismic Analysis Report”, Revision 1
f. USNRC, “Interim Staff Guidance on Ensuring Hazard-Consistent Seismic Input for Site Response and Soil Structure Interaction Analyses”, DC/COL-ISG-017 (NRC ADAMS Accession Number ML092230543)
g. USNRC, Regulatory Guide 1.60: “Design Response Spectra for Seismic Design of Nuclear Power Plants”, Revision 2, July 2014

h. SRP 3.7.1, "Seismic Design Parameters", Revision 4, December 2014
i. SER-DMN-011, "Benchmarking of SASSI2010 MSM Results from NA3 Site-Specific SSI Analysis", Revision 1
j. Ostadan, F. and Deng, N., "SASSI2010 Version 1.0 User's Manual", May 2012
k. WG3-U73-ERD-S-0001, "North Anna 3 Control Building Seismic Analysis Report", Revision 0
l. DBR-0009791, "Soil-Structure Interaction Absolute Acceleration Transfer Functions With Respect to Outcrop Motion and Design Motion Power Spectral Densities For RB/FB SSI, CB SSI, FWSC SSI, CB-FWSC SSSI, and CB-RB/FB SSSI Analyses", Revision 3

3. SITE-SPECIFIC INPUT

3.1 Site-Specific Subsurface Properties

The site-specific evaluation of the SSSI effect of the RB/FB on the CB seismic response is based on the results of the SSSI analyses of the CB-RB/FB combined models performed for the LB partial column, UB partial column and UB full column profiles representing subgrade conditions at the CB location. These SSSI analyses use subgrade properties that are compatible to the strains generated by the site-specific design ground motion. The site-specific strain compatible dynamic properties of the in-situ rock and saprolite subgrade materials are assigned to the far-field SASSI SITE models and the excavated volume elements of SASSI HOUSE models. Reference 2-a provides the strain compatible dynamic properties of the far-field site-specific in-situ subgrade materials. The strain iterated properties are included in this report as listed in Tables 3.1-1 and 3.1-2. The layering and properties are adjusted to match the finite element discretization of the excavated volume and to meet passing frequency requirements. The adjusted subgrade profiles are listed in Tables 4.3-2 through 4.3-4 and are used as input for the CB-RB/FB SSSI analyses.

The CB-RB/FB combined SASSI HOUSE models also include near-field solid elements representing the concrete fill materials placed around the CB exterior walls and concrete fill placed below the CB and the Access Tunnel basemats. Additional near-field elements are used in the CB-RB/FB combined model for the analysis of the UB full column profile to represent the structural fill surrounding the three sides of the CB column except for the side that is adjacent to the Access Tunnel. The structural fill dynamic properties are compatible with the strains generated by the design ground motion. The dynamic properties used for the concrete fill are independent of strain, reflecting the linear elastic behavior of the concrete under the small design-earthquake-induced strains. Reference 2-a provides the dynamic properties of the structural and concrete fill materials from the site response analyses as listed in Tables 3.1-3 and 3.1-4. The adjusted layering and properties that are used as input for the SSSI analyses are listed in Tables 4.3-2 through 4.3-4. Table 3.1-5 presents the average strain-compatible shear wave velocities ($V_{s\text{-}ave}$) and shear column frequencies (f_{sc}) of the concrete fill, structural fill, and in-situ materials describing the overall dynamic properties of the subgrade materials around the CB.

The P-wave velocity of the saprolite and structural fill material located below the ground water level is set equal to or close to, but not less than, that of the water to capture the effect of ground water on P-wave velocity of the saturated soil unless the Poisson's ratio value that relates the S and P wave velocities becomes too high. A maximum value of 0.47 is used for the Poisson's ratio of the subgrade materials in this report.

3.2 Site-Specific Input Motion

Reference 2-a provides the statistically independent ground motion time histories used as the input control motion in the three orthogonal directions for each of the SSSI analyses of the CB-RB/FB combined model for the LB partial, UB partial and UB full column profiles. These ground motion time histories represent the in-column free-field motions at the CB foundation bottom elevation. These time histories are compatible with the envelope of the CB FIRS and the broadband spectra specified in RG 1.60 (Reference 2-g) anchored at 0.1 g. The in-column ground motion time histories used for the CB-RB/FB SSSI analyses are checked using the NEI method as required by ISG-017 (Reference 2-f).

Figure 3.2-1 of Reference 2-k presents the 5 percent damped acceleration response spectra (ARS), the power spectral density (PSD), and the cumulative power spectral density (CPSD) of the input acceleration time histories used for the CB-RB/FB SSSI analyses illustrating the energy content of the input motion at different frequencies. The presented PSDs are computed based on the strong motion portion of the time record of which the duration is defined by the time interval required for the Arias intensities to increase from 5 percent to 75 percent. Frequency averaging intervals of ±20 percent are applied in compliance with Standard Review Plan (SRP) 3.7.1 (Reference 2-h).

4. STRUCTURE-SOIL-STRUCTURE INTERACTION ANALYSIS

4.1 Analysis Method

The SSSI analyses of the CB-RB/FB combined model are performed using the SASSI2010 computer program and the MSM where only selected nodes of the excavated volume are specified as interaction nodes. Reference 2-i provides the benchmarking evaluations of the accuracy of the MSM solutions for the NA3 site-specific application. The SASSI2010 computer program uses finite elements with complex moduli for modeling the dynamic properties of the structure, foundation, backfill, and the excavated volume. They provide the solution for the seismic response of the structure-subgrade-structure interaction system based on the frequency domain complex response method. The lumped mass-beam models with full stiffness and OBE damping described in DCD Section 3A.5.1 (Reference 2-c) are coupled with the finite element soil model of the subgrade with the site-specific strain compatible dynamic properties. The model details are described in Section 4.3. Structural responses in terms of accelerations, ARS, member forces, and moments are computed directly from the SASSI2010 computer program results.

The SSSI analyses are performed separately for each one of the three directional components of input ground motion. The maximum co-directional seismic forces, moments, and

accelerations for each of the three ground motion time history components are combined using the Square Root of the Sum of the Squares (SRSS) method. The co-directional soil/rock reactions are combined using the absolute sum method in the time domain for calculation of lateral soil pressures. Reference 2-k provides detailed description of the methodology used to develop the lateral soil pressure.

The co-directional ISRS are combined using the SRSS method. The ISRS are developed for responses at the edges of the building by taking into account coupling effects between vertical and rocking, and between lateral and torsional motions. The procedure used for the development of the ISRS is the same as that used for the development of the ISRS from the site-specific SSI analyses of the CB standalone model.

The SSSI effects are evaluated based on the responses obtained from the CB-RB/FB combined models with full (uncracked concrete) stiffness properties and OBE structural damping values.

4.2 Structure-Soil-Structure Interaction Analysis Cases

Table 4.2-1 presents the three analysis cases considered for site-specific evaluation of the SSSI effects of the RB/FB on the CB seismic response.

The frequency step and Fast Fourier Transformation (FFT) number used for the SSSI analyses are 0.0244 Hz and 8192, respectively. Table 4.2-2 provides a list of frequencies used for each of the SSSI analyses performed for the CB-RB/FB combined model. As described in Subsection 5.1, acceleration transfer function results for the responses at key locations within the CB obtained from each analysis case are inspected to ensure that the selected frequencies of analysis provide numerically stable and accurate results.

Values of cut-off frequencies of analysis are used that are equal to or lower than the passing frequency of the SSSI model (the highest frequency of seismic waves that is adequate to be accurately transmitted through the SSSI model). The exception is the analysis case CR3 that is performed for frequencies up to 70 Hz, which is slightly higher than the S-wave passing frequency of 65 Hz of the model used for the CB-RB/FB SSSI analyses of UB full column profile. The SSSI analyses of the CB-RB/FB combined models that are performed for the three cases use cut-off frequencies of analysis that are identical to those used for the corresponding SSI analyses. This ensures that the energy content of the input motion captured by the SSSI analyses and the reference SSI analyses is the same and does not affect the SSSI evaluations. The analyses of the CB-RB/FB combined model and the CB standalone model for the LB partial column profile are performed using a cut-off frequency of 50 Hz. The analyses of the CB-RB/FB combined model and the CB standalone model for the UB full column and partial column profile are performed using a cut-off frequency of 70 Hz.

As described in Section 4.3, the passing frequency for each model is determined by the mesh size of the below-grade portion to satisfy the SASSI2010 user's manual (Reference 2-j) requirement that the size of the elements not more than 20% of the length of the shear wave passing through the modeled soil material is adequate to accurately transmit the waves.

4.3 Analysis Models

The combined models of the CB and RB/FB used for the site-specific SSSI analyses are developed from standalone CB and RB/FB three-dimensional lumped mass-stick models (LMSMs) documented in References 2-k and 2-e, respectively. The combined models also include solid elements modeling the near field concrete fill and structural fill, and shell elements modeling the Access Tunnel. The structural elements are assigned with full stiffness and OBE damping values representing uncracked reinforced concrete condition.

The CB and RB/FB SSSI analyses are performed for three subgrade profiles: LB partial column, UB partial column and UB full column. The two combined models for the SSSI analyses of the LB and UB partial column subgrade profiles have the same geometry and mesh discretization. Figure 4.3-1 presents the CB-RB/FB combined models with LB or UB partial column and UB full column (subgrade profiles. The model axes in X-direction and Y-direction represent plant NS direction and EW direction of NA3 site, respectively. The Z axis represents the vertical direction). The SSSI analyses of CB-RB/FB combined model are performed using soil profiles and input ground motion representing the conditions at the CB because the primary focus of the study is on how the heavy RB/FB affects the response of the light, deeply embedded CB.

The configuration of the CB in the CB-RB/FB combined model is as close as possible to that of the standalone CB model used for Licensing Basis analyses in Reference 2-k. The structural models and excavated volume models for the CB-RB/FB combined model are shown in Figures 4.3-2 through 4.3-4. The configuration of the RB/FB is adjusted to reduce the size of the combined model. As shown in Figure 4.3-2, the RB/FB stick model basemat mass nodes are moved 0.42 m north in order to match the meshing of the CB model. The elevation of rigid beams installed in shell walls are also adjusted as shown in Figures 4.3-3 and 4.3-4. The adjustment of the RB/FB is small and does not impact the overall dynamic properties of RB/FB. The bottom of the combined CB-RB/FB structural model and the top of the Zone III rock is established at the RB/FB basemat bottom elevation of -15.5 m.

In order to accurately capture the SSSI effects through the embedment soil and rock, the combined model provides a close representation of the actual plant layout and the embedment conditions existing between the CB and RB/FB. Unlike the standalone fully embedded models of RB/FB and CB, the combined CB-RB/FB model does not include structural fill elements in the space between the RB/FB and the CB to account for the presence of the Access Tunnel that is seismically isolated from the RB/FB and CB walls. Solid elements are used to model the concrete and structural fill around the other three sides of the CB to capture the effect of the backfilled materials on the CB SSSI response. The concrete and structural fill around the other three sides of the RB/FB are not included in the combined model since their effect on the CB response is small.

In the combined SSSI model, the Access Tunnel is modeled by shell elements representing the dynamic properties of the two exterior walls facing the RB/FB and CB, the two interior walls, the roof slab, basemat and one intermediate slab as shown in Figures 4.3-2 through 4.3-4. The model is based on the conceptual design drawings of the Access Tunnel and has

the sole purpose of representing the overall dynamic properties of this structure. The elevations of the Access Tunnel intermediate slab and the basemat match the meshing of the CB and RB/FB. The Access Tunnel intermediate slab and the basemat are at EL 1.2 m and EL -3.12 m, respectively. The center planes of the Access Tunnel exterior walls are assumed to be at the same locations as the CB or RB/FB below-grade exterior walls. The Access Tunnel model shares the same nodes with the concrete fill at the bottom. Since there are seismic gaps between the Access Tunnel and adjacent buildings, the exterior walls of the Access Tunnel are not connected to the CB and RB/FB. Similar to the stand-alone models, the staircases between the Access Tunnel and the CB or RB/FB are neglected. The reinforced concrete unit weight of 2.4 t/m^3 is assigned to Access Tunnel shell elements. The thickness and material properties assigned to Access Tunnel structural members are presented in Table 4.3-1.

The CB and RB/FB below-grade exterior walls and the CB-RB/FB foundation basemats are modeled using plate elements similar to the standalone CB and RB/FB SASSI models used for standard design (DCD) SSI analyses. However, because the soil medium between the top of the plant grade or Zone III rock and the foundation basemat are modeled in the NA3 site-specific SSSI analyses, the vertical spacing of the wall nodes is adjusted to match the site-specific subsurface layers that meet the passing frequency requirements. The sizes of the plate elements are also adjusted to satisfy the SASSI2010 requirement for the mesh size that limits the size of the elements to not more than 20 percent of the length of the shear wave with cut-off frequency passing through the soil material. Massless shell elements are used with thickness set as a quarter of the corresponding basemat width to represent the in-plane stiffness of the CB basemat from EL -7.4 m to -10.4 m and the RB/FB basemat from EL -11.5 m to -15.5 m.

The mesh size of the excavated volume elements is refined enough to ensure that per SASSI2010 criteria, the maximum element size in all three directions does not exceed 20 percent of the shear wave length of the excavated soil at the highest (cut-off) frequency of analysis. The backfill surrounding CB is included in the structural models and is modeled using 3-D solid elements with mesh that is consistent with the mesh of the plate elements of the basemat and exterior walls. For the full column or fully embedded (FE) UB model, a refined mesh is required for the top layers of softer in-situ soil and structural fill located above the Zone III rock in the SSSI analysis in order to capture sufficient energy of the design input motion. To ensure the overall model size does not exceed the program limitations, the soil medium and concrete fill below the Zone III rock level are modeled with coarser mesh. In the transitional layers, non-uniform irregular elements are used, namely, triangular shell elements, prism, tetrahedral, and pyramid solid elements. The combined models' passing frequencies and cut-off frequencies used for the CB-RB/FB SSSI analyses are shown in Table 4.2-1. The passing frequencies are calculated on the basis of both the maximum horizontal and vertical dimensions of the excavated volume and backfill mesh. The table shows that the model maximum passing frequencies for all subsurface profiles are not smaller than the cut-off frequency of analysis except for fully embedded UB subgrade profiles as described in Section 4.2. The SSSI analysis of partial column or partially

embedded LB and UB, and full column or fully embedded UB subgrade profiles capture at least 97%, 99% and 95% of the input motion energy, respectively.

The maximum aspect ratio of the regular 3-D thin shell elements in the CB-RB/FB partially embedded and fully embedded models are 1:1.7, 1:2.0, respectively. The maximum aspect ratio of the regular 3-D solid brick elements in the CB-RB/FB partially embedded and fully embedded models are 1:1.5, 1:2.3, respectively. The accuracy of the SASSI2010 program has been verified and validated for models with a maximum aspect ratio of 1:4 for both the 3-D thin shell and 3-D solid brick finite elements. Additionally, the accuracy of using non-uniform irregular elements is also demonstrated for the CB standalone model SSI analysis by a comparative study as shown in Reference 2-k.

The site profiles used for the site-specific CB-RB/FB SSSI analyses are presented in Tables 4.3-2 through 4.3-4. The maximum value of soil Poisson's ratio considered in the site models is 0.47 which is within the range to which the accuracy of SASSI2010 program has been verified and validated. The shear and compression wave velocities, unit weights, and damping ratios of the profiles used for the SSSI analyses are derived from those provided in the strain iterated soil profiles listed in Tables 3.1-1 and 3.1-2 developed from the results of the site response analysis. Some of the layers in these site response analysis profiles are divided or combined so the site models used for site-specific SSSI analyses can meet the passing frequency requirements and the layering matches the FE discretization of the excavated volume. A graphical comparison between the adjusted soil profiles of shear wave velocities, compression wave velocities and damping ratios used in the SSSI analyses and the corresponding strain iterated soil profiles from the site response analyses are provided in Figures 4.3-6 and 4.3-7.

The CB-RB/FB partially embedded LB and UB, and fully embedded UB site models include 67, 67 and 75 layers on top of a half-space, respectively. The top of the half-space in the SSSI model is established at DCD elevation -196.5 m. Consistent with SASSI manual recommendations (Reference 2-j), the half-space simulation consists of additional ten layers with viscous dashpots added at the base of the site finite element model to account for the dissipation of energy at the model lower boundary. The total depth of the site model used for SSSI analyses is more than 195 m, which exceeds two times the footprint dimension of the analyzed structures.

The CB-RB/FB full column and partial column excavated volume models are shown in Figures 4.3-3 and 4.3-4, respectively. The selection of the interaction nodes is based on the conclusions of the MSM benchmarking report (Reference 2-i). In addition to the nodes at the sides, top and bottom surfaces of the excavated volumes of the CB and RB/FB, nodes at vertical plane between CB and RB/FB and nodes at two horizontal planes within the excavated volumes are added as interaction nodes for both models.

As indicated in Figures 4.3-3 and 4.3-4, the CB stick model is connected to the basemat and side walls at floor EL -7.4 m, -2.0 m, and 4.5 m by a set of rigid beams. Likewise, the RB/FB stick model is also connected to the side walls at floor EL -11.5 m, -6.17 m, -1.0 m, and 4.5

m by a set of rigid beams. At the base of the model at EL -15.5 m, a rigid link is used to connect all the RB/FB sticks to the center of the basemat.

In the CB-RB/FB model, 3-D spring elements which have stiffness in three directions are established at the CB exterior wall/backfill interfaces and concrete fill under the CB basemat as shown in Figure 4.3-5. 3-D spring elements are also established at the interfaces around the RB/FB exterior walls and basemat with the in-situ soil and concrete fill. These spring elements are assigned global stiffness properties high enough to ensure they do not affect the dynamic properties of the analyzed SSSI system. The interface spring elements provide spring force results that serve as input for calculation of the site-specific wall lateral pressure and foundation bearing pressure demands.

5. EVALUATION OF RB/FB SSSI EFFECTS ON CB SEIMIC RESPONSE

This section presents the results of the site-specific evaluation of SSSI effects of the RB/FB on the CB seismic response. The evaluation is based on the comparison of the results of the site-specific SSSI analyses of the CB-RB/FB combined model listed in Table 4.2-1 for the response of the CB with the corresponding results obtained from the site-specific SSI analyses of the standalone CB models for the LB and UB partial column, and UB full column profiles. Plots of the calculated and interpolated acceleration transfer function results for the responses of the CB are used to demonstrate the accuracy of the interpolated results from the SSSI analyses of the three subgrade stiffness cases. The SSSI effects of the RB/FB on the CB seismic response are evaluated by comparing the results for maximum accelerations, maximum member forces, maximum lateral pressures on below-grade exterior walls, and ISRS.

The RB/FB SSSI effects on the CB site-specific seismic design basis are evaluated by comparing the site-specific CB-RB/FB SSSI analysis results with the corresponding CB site-specific seismic design basis ISRS that are developed in Reference 2-k as the envelope of the results of the SSI analyses of the CB standalone models. The maximum seismic responses, namely, maximum accelerations, maximum member forces, and maximum lateral pressures on below-grade exterior walls are compared with the responses that are developed as the envelope of the SSI analyses of the CB standalone models for the cases of full stiffness (uncracked reinforced concrete) and OBE damping values. Comparisons are also made with the corresponding seismic loads and ISRS used for the standard design of the CB that are documented in Reference 2-d to further evaluate the significance of the site-specific SSSI effects.

5.1 Acceleration Transfer Function Results

Appendix B presents plots of the amplitudes of the acceleration transfer functions obtained directly from the SASSI2010 computer program analyses, which represent the responses at the following key locations within the CB relative to the in-layer seismic input motion:

Location	Node Number	SASSI Model Node Number
CB Top	6	500
CB Basemat	2	410

The amplitudes of the acceleration transfer functions are presented from the analyses of the partial column LB and UB, and full column UB subgrade profiles. Each figure presented in Appendix B includes three plots presenting the CB responses in the three orthogonal directions due to the three earthquake components. The computed values of the transfer functions in these plots are depicted with dots. The interpolated values of the transfer functions are depicted by solid lines.

As expected, the acceleration transfer functions for the horizontal response of the CB are characterized with large peaks at frequencies that are close to the embedment shear column frequencies listed in Table 3.1-5 and at frequencies where dips occur in the response spectra of the input in-layer acceleration time histories presented in Figure 3.2-1. Therefore, these large peaks in the acceleration transfer functions that represent the response amplifications relative to the in-column input motion are generally not reflected in the acceleration response spectra results.

The plots shown in Appendix B generally have no numerical anomalies in the interpolated transfer functions (e.g., sharp narrow spikes) that can potentially impact the accuracy of the frequency domain SSSI analyses results. This observation confirms further that the solution is stable, and the MSM and selection of the interaction nodes used in the analyses produce reasonable responses. The isolated sharp peak in a few cases does not affect the accuracy of the corresponding responses.

The large peaks at soil column frequencies are generally not present in the transfer functions representing the structural responses relative to the input outcrop motion making them a better indicator of structural response. These outcrop transfer functions are calculated in the following three steps:

1. FFT are performed on the time histories of in-layer and outcrop ground motion at the CB basemat bottom elevation obtained from Reference 2-b.
2. The ratio between the in-layer and outcrop motion Fourier Transforms yields transfer functions representing the transformation of the CB in-layer motion into an outcrop motion.
3. The product of the complex in-layer/outcrop transfer functions calculated in step 2 and the SASSI2010 calculated complex transfer functions of the structural response relative to the in-column motion provides the transfer functions for the response of the CB relative to the outcrop motion.

Reference 2-l documents the calculations of the transfer functions relative to the outcrop motion. Figure 5.1-1 presents amplitudes of the transfer functions representing the transformation of the in-layer motion time histories used as input for the CB-RB/FB SSSI analysis of the UB full, LB and UB partial column profiles into the corresponding horizontal and vertical design outcrop motion time histories. The first valleys in the horizontal full

column motion in-layer/outcrop transfer functions occur at frequencies close to the rock/soil embedment shear column frequencies listed in Table 3.1-5.

Figure 5.1-2 presents the outcrop transfer function amplitudes for the co-directional responses of the CB top (Node 6) in the NS (X), EW (Y), and vertical (Z) directions obtained from the analyses of LB and UB partial column and UB full column profiles. Figure 5.1-3 presents the outcrop transfer functions amplitudes for the rotational accelerations that are representative of the rocking responses along the NS (X) and EW (Y) directions at the top of CB basemat (Node 2) due to vertical (Z) component. The plots compare the results from the site-specific SSSI analyses of the CB-RB/FB combined model presented by dashed lines with the results from the site-specific SSI analyses of the CB standalone model presented with solid lines. Comparisons are shown for the outcrop transfer function results obtained from the analyses of LB partial column and UB full column profiles to illustrate the effects of the subgrade stiffness on the SSSI responses. The plots also show the outcrop motion design spectra (FIRS) for the partial column and full column with solid and dashed lines, respectively.

The comparisons in Figure 5.1-2 show that generally the SSSI effects on the horizontal and vertical peak responses of the CB are small without any significant shifts in the peak response frequencies. Figure 5.1-3 indicates that the SSSI effects of RB/FB amplifies the rocking response of the CB basemat. These transfer function plots show that the softer LB subgrade properties amplify the SSSI effects of the RB/FB on the CB rocking response. The plots also show that the saprolite and engineered fill embedment also can amplify the rocking response of the CB along the EW (Y) direction.

5.2 SSSI Effects of RB/FB on CB Maximum Responses

Figure 5.2-1 presents comparisons of the results for maximum absolute accelerations at CB mass locations from the site-specific SSSI analyses of CB-RB/FB combined model with the corresponding results from the site-specific SSI analyses of the CB standalone model for the UB full, LB and UB partial column profiles. Table 5.2-1 shows the comparison of the results from the SSSI analyses of the CB-RB/FB combined model and the SSI analyses of the CB standalone model for maximum accelerations of the Single Degree of Freedom (SDOF) oscillators representing the out-of-plane vibrations of the CB flexible slabs. Figure 5.2-2 presents the comparisons of the results for maximum shear forces and torsion from the SSSI analyses of the CB-RB/FB combined model with the corresponding results from the SSI analyses of the CB standalone model for the UB full, LB and UB partial column profiles. The figures show the results from the CB-RB/FB SSSI analyses with red dashed lines. The results obtained from the SSI analyses of the CB standalone model are shown with green solid lines.

The comparisons in Figures 5.2-1 and 5.2-2 show that the SSSI effects generally slightly amplify the Y and Z direction responses while reducing X direction responses. As shown in Figure 5.2-1, the SSSI of the RB/FB has significant effect only on the CB torsional response. These torsional moment amplifications are induced by the eccentricity of the RB/FB with respect to both the NS axis and the EW axis. Amplifications of the CB horizontal and vertical responses are observed only in the results obtained from the CB-RB/FB SSSI

analyses of the LB partial and UB full column subgrade profiles. These amplifications are enveloped by the results of the SSI analyses of the standalone CB model for the UB partial column subgrade profile. The comparisons in Table 5.2-1 show that the SSSI effects on the maximum vertical accelerations of the CB flexible slabs (SDOFs) are small. The SSSI effects can either slightly amplify or reduce the maximum accelerations of the CB slab oscillators.

5.3 SSSI Effects of RB/FB on Dynamic Lateral Pressures on CB Below-Grade Walls

As discussed in Section 4.3, spring elements between "double nodes" are installed on the CB wall interfaces with surrounding subgrade to calculate the lateral seismic pressures on the CB below-grade walls. The calculations of dynamic lateral pressures are performed in the following steps:

1. The time histories of the spring forces are extracted from each SASSI run for each contact spring element.
2. The absolute value of the spring force magnitudes obtained from the analyses of the three orthogonal input earthquake motion components are combined absolutely in the time domain.
3. The maximum lateral forces normal to the wall plane are obtained at all contact spring elements.
4. The absolute values of the maximum lateral forces for all spring elements at the same elevations are summed up to obtain the total maximum lateral forces at the respective elevations for the three CB below-grade exterior walls separately.
5. The total maximum lateral forces are divided by the tributary area for each node group at the same elevation to obtain the soil pressure distribution for the four exterior walls.

Figures 5.3-1 and 5.3-2 present the SASSI calculated dynamic lateral pressures on the CB below-grade walls located at column lines C1 (North Wall) and C5 (South Wall). Figures 5.3-3 and 5.3-4 present the dynamic lateral pressures on the CB below-grade walls located at column lines CA (East Wall) and CD (West Wall), respectively. The figures compare the dynamic lateral pressures obtained from the site-specific SSSI analyses of the CB-RB/FB combined model that are presented with dashed red lines with the corresponding dynamic lateral pressures obtained from the site-specific SSI analyses of the CB standalone model that are presented with solid green lines. Comparisons are presented of the results obtained from the SSSI and SSI analyses of the LB and UB partial column and UB full column profiles with the envelope of the results obtained from the SSI analyses of the CB standalone model with full stiffness properties and OBE damping in Reference 2-k.

The figures show that the effects of presence of the RB/FB on dynamic lateral pressures on CB walls C1, C5 and CA are minimal. Compared to the results from standalone SSI analysis, exceedance due to SSSI effects is shown for the CB-CD wall (West Wall) facing the RB/FB. The exceedance occurs at the top level of in-situ rock (EL -3.12 m) and at the basemat level (about EL -10.4 m).

5.4 SSSI Effects of RB/FB on CB ISRS

Figures 5.4-1 through 5.4-3 present a comparison of the results from the site-specific SSSI analyses of the CB-RB/FB combined model and the site-specific SSI analyses of the CB standalone model for 5 percent damped ISRS for response in the NS, EW, and vertical directions, respectively. ISRS are presented for the CB response at the two key locations within the CB listed in Section 5.1. The following is the procedure used for the development of the floor ISRS:

1. For each of the four outrigger locations (ne, nw, se, sw) at particular floor elevations, three components (X, Y, and Z) of the ARS due to input motion in three directions (X, Y, and Z) are calculated by the SASSI2010 MOTION module to obtain a total of 36 ARS results ($f_{XY}^{(ne)}$ means Y-directional response due to X-directional input motion at the northeast location of outrigger):

   $\text{Outrigger}^{(\text{ne})} \rightarrow (f_{XX}^{(ne)}, f_{XY}^{(ne)}, f_{XZ}^{(ne)}, f_{YX}^{(ne)}, f_{YY}^{(ne)}, f_{YZ}^{(ne)}, f_{ZX}^{(ne)}, f_{ZY}^{(ne)}, f_{ZZ}^{(ne)})$

   $\text{Outrigger}^{(\text{nw})} \rightarrow (f_{XX}^{(nw)}, f_{XY}^{(nw)}, f_{XZ}^{(nw)}, f_{YX}^{(nw)}, f_{YY}^{(nw)}, f_{YZ}^{(nw)}, f_{ZX}^{(nw)}, f_{ZY}^{(nw)}, f_{ZZ}^{(nw)})$

   $\text{Outrigger}^{(\text{se})} \rightarrow (f_{XX}^{(se)}, f_{XY}^{(se)}, f_{XZ}^{(se)}, f_{YX}^{(se)}, f_{YY}^{(se)}, f_{YZ}^{(se)}, f_{ZX}^{(se)}, f_{ZY}^{(se)}, f_{ZZ}^{(se)})$

   $\text{Outrigger}^{(\text{sw})} \rightarrow (f_{XX}^{(sw)}, f_{XY}^{(sw)}, f_{XZ}^{(sw)}, f_{YX}^{(sw)}, f_{YY}^{(sw)}, f_{YZ}^{(sw)}, f_{ZX}^{(sw)}, f_{ZY}^{(sw)}, f_{ZZ}^{(sw)})$

   where f_{ij} represent ARS in j-direction due to earthquake in i-direction

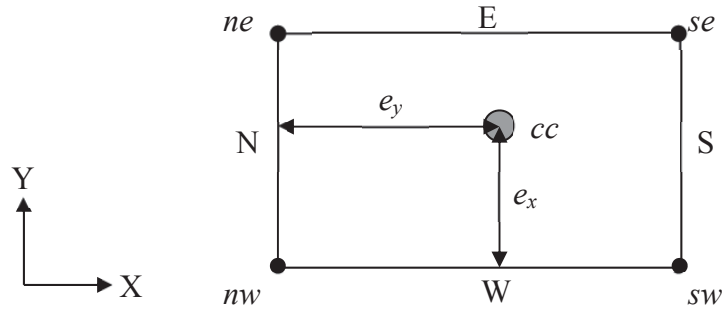

The spectra for the nodal responses due to the three input motion components in the X, Y and Z directions are combined using the SRSS method to obtain a total of 12 ARS of the response of each of the four outrigger nodes (ne, nw, se, sw) in three orthogonal directions (X, Y, and Z):

$$f_X^{(ne)} = \sqrt{f_{XX}^{(ne)2} + f_{YX}^{(ne)2} + f_{ZX}^{(ne)2}} \quad , \quad f_Y^{(ne)} = \sqrt{f_{XY}^{(ne)2} + f_{YY}^{(ne)2} + f_{ZY}^{(ne)2}}$$

$$f_Z^{(ne)} = \sqrt{f_{XZ}^{(ne)2} + f_{YZ}^{(ne)2} + f_{ZZ}^{(ne)2}}$$

$$f_X^{(nw)} = \sqrt{f_{XX}^{(nw)2} + f_{YX}^{(nw)2} + f_{ZX}^{(nw)2}} \quad , \quad f_Y^{(nw)} = \sqrt{f_{XY}^{(nw)2} + f_{YY}^{(nw)2} + f_{ZY}^{(nw)2}}$$

$$f_Z^{(nw)} = \sqrt{f_{XZ}^{(nw)2} + f_{YZ}^{(nw)2} + f_{ZZ}^{(nw)2}}$$

$$f_X^{(se)} = \sqrt{f_{XX}^{(se)2} + f_{YX}^{(se)2} + f_{ZX}^{(se)2}} \quad , \quad f_Y^{(se)} = \sqrt{f_{XY}^{(se)2} + f_{YY}^{(se)2} + f_{ZY}^{(se)2}}$$

$$f_Z^{(se)} = \sqrt{f_{XZ}^{(se)2} + f_{YZ}^{(se)2} + f_{ZZ}^{(se)2}}$$

$$f_X^{(sw)} = \sqrt{f_{XX}^{(sw)2} + f_{YX}^{(sw)2} + f_{ZX}^{(sw)2}} \quad , \quad f_Y^{(sw)} = \sqrt{f_{XY}^{(sw)2} + f_{YY}^{(sw)2} + f_{ZY}^{(sw)2}}$$

$$f_Z^{(sw)} = \sqrt{f_{XZ}^{(sw)2} + f_{YZ}^{(sw)2} + f_{ZZ}^{(sw)2}}$$

2. The ARS calculated for each outrigger location are enveloped to obtain the three ARS for the floor response in three orthogonal directions (X, Y, and Z):

$$F_X = max(f_X^{(ne)}, f_X^{(nw)}, f_X^{(se)}, f_X^{(sw)})$$

$$F_Y = max(f_Y^{(ne)}, f_Y^{(nw)}, f_Y^{(se)}, f_Y^{(sw)})$$

$$F_Z = max(f_Z^{(ne)}, f_Z^{(nw)}, f_Z^{(se)}, f_Z^{(sw)})$$

The comparison of the ISRS results in Figures 5.4-1 through 5.4-3 show that:

- The SSSI effects generally slightly increase the amplitude of the EW and vertical ISRS in the high frequency range for frequencies greater than 10 Hz.
- More pronounced amplifications of ISRS amplitudes can be noted for the EW response at the top of the basemat at frequencies between 20 and 50 Hz. These exceedances are enveloped by the corresponding standard design ISRS.
- The SSSI effects with RB/FB also amplify the vertical ISRS. The peaks of the vertical ISRS obtained from the SSSI analysis can exceed both the NA3 design basis ISRS and the standard design ISRS. The sharp peak at 25 Hz in the ISRS for the vertical response of the CB roof exceeds the corresponding NA3 site-specific design ISRS by approximately 5%. The sharp peak at 50 Hz of the ISRS representing the vertical response at the top of the CB basemat exceeds the NA3 site-specific ISRS by less than 25%.

5.5 SSSI Effects of RB/FB on Site-Specific Load Demands on CB Structure

The seismic structural loads representative of the site-specific seismic demands on the CB structure are developed following the methodology used to develop the standard design enveloping maximum structural loads presented in Reference 2-d. The horizontal load demands on the CB reinforced concrete structure are developed from the diagrams of the maximum enveloping shear forces and maximum enveloping torsional moments obtained as the envelope of the member force results from the analyses of the six subgrade profiles. The vertical site-specific seismic load demands on the CB structure are developed from the diagrams of the maximum enveloping vertical floor mass accelerations obtained as the envelope of the maximum acceleration results from the analyses of the six subgrade profiles. The maximum enveloping bending moments are also used for the structural evaluation of the CB to account for the effects of floor rocking on the wall axial forces. The results for

maximum enveloping vertical accelerations of the SDOF oscillator mass are used to develop the local out-of-plane load demands on the CB flexible slabs.

The SSSI effects of the RB/FB on the site-specific seismic load demands on the CB structure are evaluated based on the diagrams of the maximum vertical accelerations, member shear forces and moments obtained as the envelope of the results from the site-specific SSSI analyses of the CB-RB/FB combined model for the LB and UB partial column, and UB full column profiles. Figures 5.5-1 and 5.5-2 compare the envelopes of the SSSI results with the corresponding diagrams of enveloping site-specific maximum horizontal and vertical load demands obtained as envelopes of the results of site-specific SSI analysis of the CB standalone model (Reference 2-k) for:

i. LB partial column profile
ii. UB partial column profile
iii. UB full column profile

The figures present the envelope of the SSSI results with solid red lines and the NA3 enveloping seismic demands from the CB site-specific SSI analyses with solid green lines. Figures 5.5-1 and 5.5-2 also provide, with dashed blue lines, the diagrams of the horizontal and vertical seismic loads used for the standard design of the CB reinforced concrete structures.

Table 5.5-1 compares the envelope of the site-specific SSSI analyses results of the three cases for maximum accelerations at the CB floor mass locations with the corresponding NA3 enveloping maximum accelerations obtained from the SSI analyses of the CB standalone model and the standard design enveloping maximum accelerations. Table 5.2-1 presents comparisons of the envelope of the SSSI analyses results for the maximum acceleration of the slab SDOF oscillators with corresponding NA3 SSI enveloping and standard design values. The comparisons of the envelope of the site-specific SSSI analyses results for maximum member forces and moments with the corresponding standard design and NA3 SSI enveloping values is presented in Table 5.5-2. Figures 5.3-1 through 5.3-4 compare the site-specific SSSI analyses results for dynamic lateral pressures with the corresponding NA3 enveloping dynamic pressures obtained from the SSI analyses of the CB standalone model.

The comparisons show that the site-specific enveloping load demands, which are obtained as the envelope of the SSI analysis results that consider both full and partial embedment configurations, envelope the SSSI effects of the RB/FB on the CB seismic response. The only exception is the torsional demands on the CB that are induced by the eccentricity of the RB/FB with respect to both the NS axis and the EW axis. The calculations in Table 5.5-3 demonstrate that the additional shear load demands induced by these SSSI amplification of the CB torsional response are enveloped by the shear load demands obtained from the site-specific SSI analyses of the CB standalone model.

The SSSI induced exceedances of the vertical load demands (maximum vertical accelerations and bending moments) on the CB walls shown in Tables 5.5-1 and 5.5-2 are negligibly small (< 2%). Table 5.5-4 presents comparison of the out-of-plane loads on the CB flexible slabs that are based on the results of the CB-RB/FB SSSI and the CB SSI analyses performed for

the UB partial column profile. The out-of-plane loads on the CB flexible slabs are calculated following the methodology described in Appendix D of Reference 2-k. The comparison shows that the SSSI induced amplifications of the out-of-plane load demands on the CB flexible slabs are negligibly small (< 3%).

The comparisons in Figures 5.3-1 through 5.3-4 of the dynamic lateral pressures show that the envelope of the results from the SSI analyses of the CB standalone model provide dynamic lateral pressures that envelope the SSSI effects of RB/FB on the CB seismic response. The only exceptions are the lateral pressures on the CB west wall facing the RB/FB. As shown in Figure 5.3-4, the lateral pressures on the CB west wall that are obtained from the CB-RB/FB SSSI analysis of the UB partial column exceed the envelope of the SSI analyses lateral pressures results. The only significant exceedance that can be observed at the bottom level of the basemat has no effects on the CB below-grade wall design. The CB west wall is supported at the floor level at EL -2.0 m, so the relatively small exceedance of the dynamic lateral pressure demand at the rock EL -3.12 m has negligibly small effect on the out-of-plane flexural and shear stress demands on the CB west exterior wall.

The NA3 site-specific seismic load demands on the CB structures presented in this section are based on the models with full concrete stiffness (uncracked) and OBE damping values in both SSI and SSSI analyses.

5.6 SSSI Effects of RB/FB on CB Site-Specific Design ISRS

Figures 5.4-1 through 5.4-3 provide a comparison of the 5% damped ISRS obtained from the site-specific SSSI analyses of the CB-RB/FB combined model with the corresponding 5% damped NA3 site-specific design and standard design ISRS shown with thick blue and black lines, respectively. The NA3 site-specific design ISRS that are broadened by ±15% and valley filled, represent the envelope of the ISRS results from the site-specific SSI analyses of the CB standalone model and serve as the basis for the site-specific design and qualification of CB equipment and components. The comparisons show that the ISRS representing the EW response at the top of the CB basemat obtained from the SSSI analyses of UB partial and full column profiles exceed the corresponding NA3 site-specific ISRS at frequencies greater than 30 Hz. The effect these exceedances have on the design are neglected because the standard-design ISRS for the horizontal response at the top of the CB basemat envelope the ISRS obtained from the site-specific SSI and SSSI analyses. The SSSI induced sharp peak exceedance of the ISRS for the vertical response at the top of CB basemat occurs at a high frequency of 50 Hz. This high frequency exceedance will be offset if the effects of the incoherence ground motion are considered.

6. CONCLUSIONS

The results of the evaluations presented in this report show that the SSSI between the CB and the RB/FB have small effect on the site-specific seismic response of CB at NA3 site. The CB site-specific design developed in Reference 2-k is based on the envelope of the results obtained from the SSI analyses of the CB standalone models representing two bounding embedment conditions:

- Partially embedded in Zone III rock that neglects the effects of the structural fill and in-situ saprolite on the seismic response of the CB
- Fully embedded that includes the effects of the structural fill and in-situ saprolite on the seismic response of the CB

The consideration of these two bounding embedment conditions provides a site-specific design basis along with the standard design basis that bounds the possible amplifications of the CB seismic response due to SSSI effects from the nearby RB/FB.

The NA3 site-specific enveloping load demands on CB structure presented in Section 6.1 of Reference 2-k envelope the SSSI effects of RB/FB on the CB seismic response with very small local exceedances that can be neglected. The results of this evaluation show that the SSSI effects of RB/FB can amplify the peaks of some of the CB ISRS. The effect of these exceedances can be neglected because they are either bounded by the standard design or occur at high frequencies (≈ 50 Hz) where they could be offset if the effect of incoherent ground motion is considered.

Table 3.1-1 LB In-Situ Subsurface Properties at CB Location

Layer #	Thickness (m)	Top-Depth (m)	Unit Weight (t/m^3)	V_s (m/s)	V_p (m/s)	Damping (%)
1	0.76	0.00	2.00	180	365	4.83
2	0.76	0.76	2.00	180	365	4.83
3	0.76	1.52	2.00	186	782	7.42
4	0.76	2.29	2.00	186	949	7.42
5	0.76	3.05	2.00	186	949	7.42
6	0.76	3.81	2.00	186	949	7.42
7	0.76	4.57	2.08	302	1463	6.53
8	0.76	5.33	2.08	302	1463	6.53
9	0.76	6.10	2.08	302	1463	6.53
10	0.76	6.86	2.08	302	1463	6.53
11	0.76	7.62	2.32	471	1463	1.06
12	0.76	8.38	2.32	471	1463	1.06
13	0.76	9.14	2.32	471	1463	1.06
14	0.76	9.91	2.32	471	1463	1.06
15	0.76	10.67	2.32	561	1715	1.14
16	0.76	11.43	2.32	561	1715	1.14
17	0.76	12.19	2.32	561	1715	1.14
18	0.76	12.95	2.32	561	1715	1.14
19	0.76	13.72	2.32	561	1715	1.14
20	0.46	14.48	2.32	561	1715	1.14
21	1.07	14.94	2.32	561	1715	1.14
22	0.76	16.00	2.32	561	1715	1.14
23	0.76	16.76	2.32	662	2022	0.96
24	0.76	17.53	2.32	662	2022	0.96
25	0.76	18.29	2.32	662	2022	0.96
26	0.76	19.05	2.32	662	2022	0.96
27	0.30	19.81	2.61	1613	3450	1.82
28	0.91	20.12	2.61	1613	3450	1.82
29	0.91	21.03	2.61	1613	3450	1.82
30	0.91	21.95	2.61	1613	3450	1.82
31	0.91	22.86	2.61	1738	3488	1.82
32	0.61	23.77	2.61	1738	3488	1.82
33	1.52	24.38	2.61	1738	3488	1.82
34	1.52	25.91	2.61	1738	3488	1.82
35	1.52	27.43	2.61	1738	3488	1.82
36	1.52	28.96	2.61	1977	3767	1.82
37	1.52	30.48	2.61	1977	3767	1.82
38	1.52	32.00	2.63	2154	3897	1.82
39	1.52	33.53	2.63	2154	3897	1.82
40	1.52	35.05	2.63	2051	3909	1.82
41	1.52	36.58	2.63	2051	3909	1.82
42	1.52	38.10	2.63	2155	4031	1.82
43	1.52	39.62	2.63	2155	4031	1.82
44	1.52	41.15	2.63	2195	3855	1.82
45	1.52	42.67	2.63	2195	3855	1.82
46	1.52	44.20	2.63	2324	4205	1.82
47	1.52	45.72	2.63	2324	4205	1.82
48	1.52	47.24	2.63	2289	4282	1.82
49	1.52	48.77	2.63	2289	4282	1.82
50	-	50.29	2.63	2290	3915	1.82

Table 3.1-2 UB In-Situ Subsurface Properties at CB Location

Layer #	Thickness (m)	Top-Depth (m)	Unit Weight (t/m^3)	V_s (m/s)	V_p (m/s)	Damping (%)
1	0.76	0.00	2.00	394	800	1.60
2	0.76	0.76	2.00	394	800	1.60
3	0.76	1.52	2.00	506	2126	2.08
4	0.76	2.29	2.00	506	2126	2.08
5	0.76	3.05	2.00	506	2126	2.08
6	0.76	3.81	2.00	506	2126	2.08
7	0.76	4.57	2.08	621	2608	2.19
8	0.76	5.33	2.08	621	2608	2.19
9	0.76	6.10	2.08	621	2608	2.19
10	0.76	6.86	2.08	621	2608	2.19
11	0.76	7.62	2.32	808	2469	0.36
12	0.76	8.38	2.32	808	2469	0.36
13	0.76	9.14	2.32	808	2469	0.36
14	0.76	9.91	2.32	808	2469	0.36
15	0.76	10.67	2.32	1014	3098	0.35
16	0.76	11.43	2.32	1014	3098	0.35
17	0.76	12.19	2.32	1014	3098	0.35
18	0.76	12.95	2.32	1014	3098	0.35
19	0.76	13.72	2.32	1014	3098	0.35
20	0.46	14.48	2.32	1014	3098	0.35
21	1.07	14.94	2.32	1014	3098	0.35
22	0.76	16.00	2.32	1014	3098	0.35
23	0.76	16.76	2.32	993	3034	0.29
24	0.76	17.53	2.32	993	3034	0.29
25	0.76	18.29	2.32	993	3034	0.29
26	0.76	19.05	2.32	993	3034	0.29
27	0.30	19.81	2.61	2420	5174	0.55
28	0.91	20.12	2.61	2420	5174	0.55
29	0.91	21.03	2.61	2420	5174	0.55
30	0.91	21.95	2.61	2420	5174	0.55
31	0.91	22.86	2.61	2607	5233	0.55
32	0.61	23.77	2.61	2607	5233	0.55
33	1.52	24.38	2.61	2607	5233	0.55
34	1.52	25.91	2.61	2607	5233	0.55
35	1.52	27.43	2.61	2607	5233	0.55
36	1.52	28.96	2.61	2965	5650	0.55
37	1.52	30.48	2.61	2965	5650	0.55
38	1.52	32.00	2.63	3231	5845	0.55
39	1.52	33.53	2.63	3231	5845	0.55
40	1.52	35.05	2.63	3077	5863	0.55
41	1.52	36.58	2.63	3077	5863	0.55
42	1.52	38.10	2.63	3232	6047	0.55
43	1.52	39.62	2.63	3232	6047	0.55
44	1.52	41.15	2.63	3293	5783	0.55
45	1.52	42.67	2.63	3293	5783	0.55
46	1.52	44.20	2.63	3487	6308	0.55
47	1.52	45.72	2.63	3487	6308	0.55
48	1.52	47.24	2.63	3434	6424	0.55
49	1.52	48.77	2.63	3434	6424	0.55
50	-	50.29	2.63	3434	5872	0.55

Table 3.1-3 LB Properties of Structural and Concrete Fill at CB Location

Layer #	Thickness (m)	Top-Depth (m)	Unit Weight (t/m^3)	V_s (m/s)	V_p (m/s)	Damping (%)
1	0.76	0.00	2.08	134	251	4.98
2	0.76	0.76	2.08	134	251	4.98
3	0.76	1.52	2.08	148	277	7.17
4	0.76	2.29	2.08	148	755	7.17
5	0.76	3.05	2.08	146	742	8.38
6	0.76	3.81	2.08	146	742	8.38
7	0.76	4.57	2.08	150	764	9.11
8	0.76	5.33	2.08	150	764	9.11
9	0.76	6.10	2.08	157	800	8.93
10	0.76	6.86	2.08	157	800	8.93
Concrete Fill		7.62	2.32	1829	2850	1.80

Table 3.1-4 UB Properties of Structural and Concrete Fill at CB Location

Layer #	Thickness (m)	Top-Depth (m)	Unit Weight (t/m^3)	V_s (m/s)	V_p (m/s)	Damping (%)
1	0.76	0.00	2.08	292	546	1.98
2	0.76	0.76	2.08	292	546	1.98
3	0.76	1.52	2.08	350	655	2.72
4	0.76	2.29	2.08	350	1463	2.72
5	0.76	3.05	2.08	360	1463	3.24
6	0.76	3.81	2.08	360	1463	3.24
7	0.76	4.57	2.08	358	1463	3.84
8	0.76	5.33	2.08	358	1463	3.84
9	0.76	6.10	2.08	391	1463	3.60
10	0.76	6.86	2.08	391	1463	3.60
Concrete Fill		7.62	2.32	2438	3800	0.55

Table 3.1-5 Average Strain-Compatible Shear Wave Velocities and Shear Column Frequencies of the Fill and In-Situ Materials at CB Location

Soil Case	Concrete Fill/ Zone III Rock Embedment					Structural Fill/ Saprolite Embedment				
	Depth	Backfill		In-Situ		Depth	Backfill		In-Situ	
		$V_{s\text{-}ave}$	f_{sc}	$V_{s\text{-}ave}$	f_{sc}		$V_{s\text{-}ave}$	f_{sc}	$V_{s\text{-}ave}$	f_{sc}
	m	m/s	Hz	m/s	Hz	m	m/s	Hz	m/s	Hz
LB	7.3	1829	62.8	520	17.8	7.6	147	4.8	218	7.2
UB		2438	83.7	917	31.4		347	11.4	515	16.9

Table 4.2-1 CB-RB/FB Site-Specific SSSI Analysis Cases, Passing, and Cut-off Frequencies

Case No.	Subgrade Profile		Method	Control Motion El.	Passing Freq.	Cut-off Freq.	Captured Motion Energy		
					(Hz)	(Hz)	X (NS)	Y (EW)	Z (Vert.)
CR1	Partial Column	LB	MSM	241 ft	55	50	97%	97%	99%
CR2		UB			85	70	100%	100%	99%
CR3	Full Column	UB			65	70*	96%	95%	98%

* The cut-off frequency is taken as 70 Hz in order to use the same cut-off frequency as the SSI analysis of the standalone model for comparison.

Table 4.2-2 List of Frequencies for SSSI Analyses

UB FE		LB PE		UB PE	
Frequency No.	Frequency (Hz)	Frequency No.	Frequency (Hz)	Frequency No.	Frequency (Hz)
1	0.02441	1	0.02440	1	0.024414
41	1.00098	41	1.00100	41	1.000977
82	2.00195	82	2.00200	82	2.001953
123	3.00293	123	3.00290	123	3.002930
164	4.00391	164	4.00390	164	4.003906
205	5.00488	205	5.00490	205	5.004883
246	6.00586	246	6.00590	246	6.005859
287	7.00684	287	7.00680	287	7.006836
328	8.00781	328	8.00780	328	8.007813
348	8.49609	369	9.00880	369	9.008789
369	9.00879	410	10.00980	410	10.009766
389	9.49707	451	11.01070	451	11.010742
410	10.00977	492	12.01170	492	12.011719
430	10.49805	532	12.98830	532	12.988281
451	11.01074	573	13.98930	573	13.989258
471	11.49902	614	14.99020	614	14.990234
492	12.01172	655	15.99120	655	15.991211
512	12.50000	696	16.99220	696	16.992188
532	12.98828	737	17.99320	737	17.993164
552	13.47656	778	18.99410	778	18.994141
573	13.98926	819	19.99510	819	19.995117
593	14.47754	860	20.99610	860	20.996094
614	14.99023	901	21.99710	901	21.997070
634	15.47852	942	22.99800	942	22.998047
655	15.99121	983	23.99900	983	23.999023
675	16.47949	1024	25.00000	1024	25.000000
696	16.99219	1065	26.00100	1065	26.000977
737	17.99316	1106	27.00200	1106	27.001953
778	18.99414	1147	28.00290	1147	28.002930
819	19.99512	1188	29.00390	1188	29.003906
860	20.99609	1229	30.00490	1229	30.004883
901	21.99707	1270	31.00590	1270	31.005859
942	22.99805	1311	32.00680	1311	32.006836
983	23.99902	1352	33.00780	1352	33.007813
1024	25.00000	1393	34.00880	1372	33.496094
1065	26.00098	1434	35.00980	1393	34.008789
1106	27.00195	1475	36.01070	1434	35.009766
1147	28.00293	1516	37.01170	1475	36.010742
1188	29.00391	1557	38.01270	1516	37.011719
1229	30.00488	1598	39.01370	1557	38.012695
1270	31.00586	1639	40.01460	1598	39.013672
1311	32.00684	1680	41.01560	1639	40.014648
1352	33.00781	1721	42.01660	1680	41.015625
1393	34.00879	1762	43.01760	1721	42.016602
1434	35.00977	1803	44.01860	1762	43.017578
1475	36.01074	1844	45.01950	1803	44.018555
1516	37.01172	1885	46.02050	1844	45.019531
1557	38.01270	1926	47.02150	1885	46.020508
1598	39.01367	1966	47.99800	1926	47.021484
1639	40.01465	2007	48.99900	1966	47.998047
1680	41.01563	2048	50.00000	2007	48.999023
1721	42.01660			2048	50.000000
1762	43.01758			2089	51.000977
1803	44.01855			2130	52.001953
1844	45.01953			2171	53.002930
1885	46.02051			2212	54.003906
1926	47.02148			2253	55.004883
1966	47.99805			2294	56.005859

Table 4.2-2 List of Frequencies for SSSI Analyses (Continued)

UB FE		LB PE		UB PE	
Frequency No.	Frequency (Hz)	Frequency No.	Frequency (Hz)	Frequency No.	Frequency (Hz)
2007	48.999023			2335	57.006836
2048	50.000000			2376	58.007813
2089	51.000977			2417	59.008789
2130	52.001953			2458	60.009766
2171	53.002930			2499	61.010742
2212	54.003906			2540	62.011719
2253	55.004883			2581	63.012695
2294	56.005859			2622	64.013672
2335	57.006836			2663	65.014648
2376	58.007813			2703	65.991211
2417	59.008789			2744	66.992188
2458	60.009766			2785	67.993164
2499	61.010742			2826	68.994141
2540	62.011719			2867	69.995117
2581	63.012695				
2622	64.013672				
2663	65.014648				
2703	65.991211				
2744	66.992188				
2785	67.993164				
2826	68.994141				
2867	69.995117				

Table 4.3-1 Properties of Access Tunnel

Location	Thickness (mm)	Young's Modulus (t/m^2)	Unit Weight (t/m^3)	Poisson's Ratio	Damping Ratio*)
Roof Slab	500	2.53E+06	2.4	0.17	0.04
Intermediate Slab	500				
Basemat Slab	1500				
Exterior Wall	900				
Interior Wall	300				

*) The tunnel is assumed uncracked with OBE damping value.

Table 4.3-2 Subsurface Properties for CB-RB/FB SSSI Analysis of PE LB Profile

	EL	Soil						Backfill					
		Unit Weight	Vs	Vp	Damping	Highest Frequency	Poisson's	Unit Weight	Vs	Vp	Damping	Highest Frequency	Poisson's
	[m]	[t/m^3]	[m/sec]	[m/sec]	[%]	[Hz]	ratio	[t/m^3]	[m/sec]	[m/sec]	[%]	[Hz]	ratio
	-3.120	2.32	471	1463	1.06	55.4	0.442	2.32	1829	2850	1.80	215.1	0.150
	-4.645												
	-4.645	2.32	471	1463	1.06	55.4	0.442	2.32	1829	2850	1.80	215.1	0.150
	-6.170												
	-6.170	2.32	561	1715	1.14	66.0	0.440	2.32	1829	2850	1.80	215.1	0.150
	-7.400												
	-7.400	2.32	561	1715	1.14	66.0	0.440	2.32	1829	2850	1.80	215.1	0.150
	-8.900												
	-8.900	2.32	561	1715	1.14	66.0	0.440	2.32	1829	2850	1.80	215.1	0.150
	-10.400												
	-10.400	2.32	561	1715	1.14	66.0	0.440	2.32	1829	2850	1.80	215.1	0.150
	-11.500												
1	-11.500	2.32	600	1834	1.06	70.5	0.440	2.32	1829	2850	1.80	215.1	0.150
	-12.830												
	-12.830	2.32	662	2022	0.96	77.8	0.440	2.32	1829	2850	1.80	215.1	0.150
	-14.160												
2	-14.160	2.36	722	2148	1.08	84.9	0.436	2.32	1829	2850	1.80	215.1	0.150
	-15.500												
	-15.500	2.61	1613	3450	1.82	112.7	0.360						
	-18.360												
	-18.360	2.61	1738	3488	1.82	56.9	0.335						
	-24.460												
	-24.460	2.61	1977	3767	1.82	130.0	0.310						
	-27.500												
	-27.500	2.63	2154	3897	1.82	141.2	0.280						
	-30.550												
	-30.550	2.63	2051	3909	1.82	134.4	0.310						
	-33.600												
	-33.600	2.63	2155	4031	1.82	141.3	0.300						
	-36.650												
	-36.650	2.63	2195	3855	1.82	143.9	0.260						
	-39.700												
	-39.700	2.63	2324	4205	1.82	152.8	0.280						
	-42.740												
	-42.740	2.63	2289	4282	1.82	150.0	0.300						
	-45.790												
	-45.790	2.63	2290	3915	1.82		0.240						
	-												

Note: The soil properties of adjusted layer, shown red box, are evaluated from original properties shown below. In the site model, additional 48 layers with the same properties as the last layer above are added up to the half space top El. -196.5m.

Original data

1	-11.500	2.32	561	1715	1.14		0.440	2.32	1829	2850	1.80		0.150
	-12.260												
	-12.260	2.32	662	2022	0.96		0.440	2.32	1829	2850	1.80		0.150
	-12.830												
2	-14.160	2.32	662	2022	0.96		0.440	2.32	1829	2850	1.80		0.150
	-15.310												
	-15.310	2.61	1613	3450	1.82		0.360	2.32	1829	2850	1.80		0.150
	-15.500												

Table 4.3-3 Subsurface Properties for CB-RB/FB SSSI Analysis of PE UB Profile

	EL	Soil						Backfill					
		Unit Weight	Vs	Vp	Damping	Highest Frequency	Poisson's	Unit Weight	Vs	Vp	Damping	Highest Frequency	Poisson's
	[m]	[t/m^3]	[m/sec]	[m/sec]	[%]	[Hz]	ratio	[t/m^3]	[m/sec]	[m/sec]	[%]	[Hz]	ratio
	-3.120	2.32	808	2469	0.36	95.0	0.440	2.32	2438	3800	0.55	286.8	0.150
	-4.645												
	-4.645	2.32	808	2469	0.36	95.0	0.440	2.32	2438	3800	0.55	286.8	0.150
	-6.170												
	-6.170	2.32	1014	3098	0.35	119.2	0.440	2.32	2438	3800	0.55	286.8	0.150
	-7.400												
	-7.400	2.32	1014	3098	0.35	119.2	0.440	2.32	2438	3800	0.55	286.8	0.150
	-8.900												
	-8.900	2.32	1014	3098	0.35	119.2	0.440	2.32	2438	3800	0.55	286.8	0.150
	-10.400												
	-10.400	2.32	1014	3098	0.35	119.2	0.440	2.32	2438	3800	0.55	286.8	0.150
	-11.500												
1	-11.500	2.32	1005	3070	0.32	118.2	0.440	2.32	2438	3800	0.55	286.8	0.150
	-12.830												
	-12.830	2.32	993	3034	0.29	116.8	0.440	2.32	2438	3800	0.55	286.8	0.150
	-14.160												
2	-14.160	2.36	1084	3223	0.33	127.5	0.436	2.32	2438	3800	0.55	286.8	0.150
	-15.500												
	-15.500	2.61	2420	5174	0.55	169.2	0.360						
	-18.360												
	-18.360	2.61	2607	5233	0.55	85.4	0.335						
	-24.460												
	-24.460	2.61	2965	5650	0.55	195.0	0.310						
	-27.500												
	-27.500	2.63	3231	5845	0.55	211.8	0.280						
	-30.550												
	-30.550	2.63	3077	5863	0.55	201.7	0.310						
	-33.600												
	-33.600	2.63	3232	6047	0.55	211.9	0.300						
	-36.650												
	-36.650	2.63	3293	5783	0.55	215.9	0.260						
	-39.700												
	-39.700	2.63	3487	6308	0.55	229.4	0.280						
	-42.740												
	-42.740	2.63	3434	6424	0.55	225.1	0.300						
	-45.790												
	-45.790	2.63	3434	5872	0.55		0.240						
	-												

Note: The soil properties of adjusted layer, shown red box, are evaluated from original properties shown below. In the site model, additional 48 layers with the same properties as the last layer above are added up to the half space top El. -196.5m.

Original data

1	-11.500	2.32	1014	3098	0.35		0.440	2.32	2438	3800	0.55		0.150
	-12.260												
	-12.260	2.32	993	3034	0.29		0.440	2.32	2438	3800	0.55		0.150
	-12.830												
2	-14.160	2.32	993	3034	0.29		0.440	2.32	2438	3800	0.55		0.150
	-15.310												
	-15.310	2.61	2420	5174	0.55		0.360	2.32	2438	3800	0.55		0.150
	-15.500												

Table 4.3-4 Subsurface Properties for CB-RB/FB SSSI Analysis of FE UB Profile

	EL	Soil						Backfill					
		Unit Weight	Vs	Vp	Damping	Highest Frequency	Poisson's	Unit Weight	Vs	Vp	Damping	Highest Frequency	Poisson's
	[m]	[t/m^3]	[m/sec]	[m/sec]	[%]	[Hz]	ratio	[t/m^3]	[m/sec]	[m/sec]	[%]	[Hz]	ratio
	4.500	2.00	394	800	1.60	70.7	0.340	2.08	292	546	1.98	68.7	0.300
	3.740												
	3.740	2.00	394	800	1.60	70.7	0.340	2.08	292	546	1.98	68.7	0.300
	2.980												
	2.980	2.00	506	2126	2.08	90.8	0.470	2.08	350	655	2.72	82.3	0.300
	2.215												
1	2.215	2.00	506	2126	2.08	90.8	0.470	2.08	352	1463	2.85	69.3	0.469
	1.200												
	1.200	2.00	506	2126	2.08	90.8	0.470	2.08	360	1463	3.24	65.4	0.468
	0.100												
2	0.100	2.07	600	2520	2.17	107.7	0.470	2.08	358	1463	3.75	65.0	0.468
	-1.000												
3	-1.000	2.08	621	2608	2.19	111.4	0.470	2.08	371	1463	3.74	74.2	0.466
	-2.000												
	-2.000	2.08	621	2608	2.19	110.8	0.470	2.08	391	1463	3.60	69.8	0.462
	-3.120												
	-3.120	2.32	808	2469	0.36	72.5	0.440	2.32	2438	3800	0.55	286.8	0.150
	-4.645												
	-4.645	2.32	808	2469	0.36	72.5	0.440	2.32	2438	3800	0.55	286.8	0.150
	-6.170												
	-6.170	2.32	1014	3098	0.35	91.0	0.440	2.32	2438	3800	0.55	286.8	0.150
	-7.400												
	-7.400	2.32	1014	3098	0.35	91.0	0.440	2.32	2438	3800	0.55	286.8	0.150
	-8.900												
	-8.900	2.32	1014	3098	0.35	91.0	0.440	2.32	2438	3800	0.55	286.8	0.150
	-10.400												
	-10.400	2.32	1014	3098	0.35	91.0	0.440	2.32	2438	3800	0.55	286.8	0.150
	-11.500												
4	-11.500	2.32	1005	3070	0.32	90.2	0.440	2.32	2438	3800	0.55	286.8	0.150
	-12.830												
	-12.830	2.32	993	3034	0.29	89.1	0.440	2.32	2438	3800	0.55	286.8	0.150
	-14.160												
5	-14.160	2.36	1084	3223	0.33	97.3	0.436	2.32	2438	3800	0.55	286.8	0.150
	-15.500												
	-15.500	2.61	2420	5174	0.55	169.2	0.360						
	-18.360												
	-18.360	2.61	2607	5233	0.55	85.4	0.335						
	-24.460												
	-24.460	2.61	2965	5650	0.55	195.0	0.310						
	-27.500												
	-27.500	2.63	3231	5845	0.55	211.8	0.280						
	-30.550												
	-30.550	2.63	3077	5863	0.55	201.7	0.310						
	-33.600												
	-33.600	2.63	3232	6047	0.55	211.9	0.300						
	-36.650												
	-36.650	2.63	3293	5783	0.55	215.9	0.260						
	-39.700												
	-39.700	2.63	3487	6308	0.55	229.4	0.280						
	-42.740												
	-42.740	2.63	3434	6424	0.55	225.1	0.300						
	-45.790												
	-45.790	2.63	3434	5872	0.55		0.240						
	-												

Note: The soil properties of adjusted layer, shown red box, are evaluated from original properties shown below. In the site model, additional 48 layers with the same properties as the last layer above are added up to the half space top El. -196.5m.

Table 4.3-4 Subsurface Properties for CB-RB/FB SSSI Analysis of FE UB Profile (Continued)

Original data

	EL	Soil						Backfill					
		Unit Weight	Vs	Vp	Damping	Highest Frequency	Poisson's	Unit Weight	Vs	Vp	Damping	Highest Frequency	Poisson's
	[m]	[t/m^3]	[m/sec]	[m/sec]	[%]	[Hz]	ratio	[t/m^3]	[m/sec]	[m/sec]	[%]	[Hz]	ratio
1	2.215	2.00	506	2126	2.08		0.470	2.08	350	1463	2.72		0.470
	1.450												
	1.450	2.00	506	2126	2.08		0.470	2.08	360	1463	3.24		0.468
	1.200												
2	0.100	2.00	506	2126	2.08		0.470	2.08	360	1463	3.24		0.468
	-0.070												
	-0.070	2.08	621	2608	2.19		0.470	2.08	358	1463	3.84		0.468
	-1.000												
3	-1.000	2.08	621	2608	2.19		0.470	2.08	358	1463	3.84		0.468
	-1.600												
	-1.600	2.08	621	2608	2.19		0.470	2.08	391	1463	3.60		0.462
	-2.000												
4	-11.500	2.32	1014	3098	0.35		0.440	2.32	2438	3800	0.55		0.150
	-12.260												
	-12.260	2.32	993	3034	0.29		0.440	2.32	2438	3800	0.55		0.150
	-12.830												
5	-14.160	2.32	993	3034	0.29		0.440	2.32	2438	3800	0.55		0.150
	-15.310												
	-15.310	2.61	2420	5174	0.55		0.360	2.32	2438	3800	0.55		0.150
	-15.500												

Table 5.2-1 Comparison of CB Slab SDOF Oscillators Maximum Accelerations

Slab SDOF		Vertical Acceleration (g)							
		LB Partial Column Profile		UB Partial Column Profile		UB Full Column Profile		NA3 Enveloping(*)	Standard Design
Elev.	Node No.	SSI	SSSI	SSI	SSSI	SSI	SSSI		
13.80 m	9001	2.26	2.45	2.81	2.71	1.76	1.82	2.81	2.19
	9002	1.43	1.48	2.19	2.36	1.44	1.66	2.19	1.34
	9003	1.79	1.81	3.00	2.89	3.01	2.77	3.01	1.43
9.06 m	9101	2.48	2.54	2.85	2.70	2.01	2.03	2.85	2.00
	9102	1.37	1.23	1.84	1.94	1.54	1.38	1.84	1.26
	9103	1.82	1.71	2.96	2.82	3.08	2.59	3.08	1.43
4.65 m	9201	1.18	1.03	1.57	1.69	1.13	1.12	1.57	1.30
	9202	1.51	1.43	2.25	2.15	2.34	2.05	2.34	1.43
-2.00 m	9301	1.45	1.30	1.53	1.30	1.27	1.08	1.54	1.39

Note: The shaded values are exceedance from the standard design and SSI models.

(*) Envelope of results from SSI analyses of CB standalone model for LB, BE, and UB full and partial column profiles

Table 5.5-1 Comparison of Enveloping Maximum Accelerations at CB Floor Mass Locations

Elev. (m)	Node No.	Acceleration (g)								
		SSSI Analyses Envelope			NA3 Enveloping(*)			Standard Design		
		NS	EW	Vert.	NS	EW	Vert.	NS	EW	Vert.
13.80	6	1.77	1.95	1.33	1.83	2.09	1.31	1.26	1.11	1.00
9.06	5	1.35	1.41	1.19	1.41	1.51	1.18	0.88	0.90	0.86
4.65	4	0.99	1.20	0.96	1.07	1.27	0.95	0.86	0.82	0.74
-2.00	3	0.62	0.67	0.62	0.64	0.77	0.62	0.79	0.71	0.56
-7.40	2	0.45	0.43	0.63	0.48	0.43	0.64	0.54	0.54	0.51
-10.40	1	0.45	0.44	0.63	0.48	0.44	0.64	0.54	0.53	0.51

Note: The shaded values are exceedance from the standard design and SSI models.
(*) Envelope of results from SSI analyses of CB standalone model for LB, BE, and UB full and partial column profiles

Table 5.5-2 Comparison of Enveloping Maximum CB Member Forces and Moments

Element		SSSI Analyses Envelope					NA3 Enveloping Demands(*)					Standard Design				
Elev. (m)	Node No.	Shear (MN)		Bending (MN-m)		Torsion (MN-m)	Shear (MN)		Bending (MN-m)		Torsion (MN-m)	Shear (MN)		Bending (MN-m)		Torsion (MN-m)
		NS	EW	NS	EW		NS	EW	NS	EW		NS	EW	NS	EW	
13.80	6	46.4	50.0	129	116	60.8	48.0	53.8	135	108	35.0	33.1	29.1	160	124	23.1
	5			312	291				328	290				250	197	
9.06	5	84.0	85.8	413	380	112.1	86.5	92.3	435	374	73.6	53.4	54.8	360	275	44.9
	4			766	714				796	718				573	443	
4.65	4	108.0	113.9	435	263	124.7	114.5	116.9	458	263	63.0	75.6	80.1	723	540	56.9
	3			1152	908				1195	969				1136	988	
-2.00	3	46.9	49.3	608	636	81.7	51.4	55.7	652	646	33.0	124.4	99.4	1232	1036	59.9
-7.40	2			820	846				874	924				1570	1525	

Note: The shaded values are exceedance from the standard design and SSI models.
(*) Envelope of results from SSI analyses of CB standalone model for LB, BE, and UB full and partial column profiles

Table 5.5-3 Comparison of Total Shear Load Demand on CB Individual Exterior Walls

Element		SSSI Analyses Envelope		NA3 Enveloping Demands(*)		Standard Design	
Elev. (m)	Node No.	Total Shear (MN)		Total Shear (MN)		Total Shear (MN)	
		NS	EW	NS	EW	NS	EW
13.80	6	49.0	52.0	49.5	54.9	34.1	29.9
	5						
9.06	5	88.8	89.5	89.6	94.7	55.2	56.2
	4						
4.65	4	113.2	118.1	117.1	119.0	78.0	82.0
	3						
-2.00	3	50.3	52.0	52.7	56.7	126.9	101.4
-7.40	2						

(*) Envelope of results from SSI analyses of CB standalone model for LB, BE, and UB full and partial column profiles

Table 5.5-4 Comparison of Out-of Plane Load Demand on CB Flexible Slabs
(SSI and SSSI Analyses of UB Partial Column Profile)

Slab		SDOF Oscillator				Flex. Mode Acc. (g)		LMSM Mass Node	Rigid Mode Weight (kN)	Rigid Mode Acc. (g)		Eq. Ave. Acc. (g)		SSSI Exceed.
Elev. (m)	Location	Weight (kN)	Mass Node	Acc. (g)										
				SSSI	SSI	SSSI	SSI			SSSI	SSI	SSSI	SSI	
-2.00	CA-CD	4325	9301	1.30	1.53	1.30	1.53	3	32570	0.62	0.62	0.70	0.73	-
4.65	CA-CD	8022	9201	1.69	1.57	1.70	1.59	4	27986	0.96	0.95	1.13	1.10	2.8%
		227	9202	2.15	2.25									
9.06	CA-CD	3494	9101	2.70	2.85	2.31	2.32	5	19785	1.19	1.18	1.55	1.54	0.6%
		4907	9102	1.94	1.84									
		850	9103	2.82	2.96									
13.80	Roof	5478	9001	2.71	2.81	2.54	2.51	6	10745	1.33	1.31	1.99	1.96	1.5%
		6390	9002	2.36	2.19									
		781	9003	2.89	3.00									

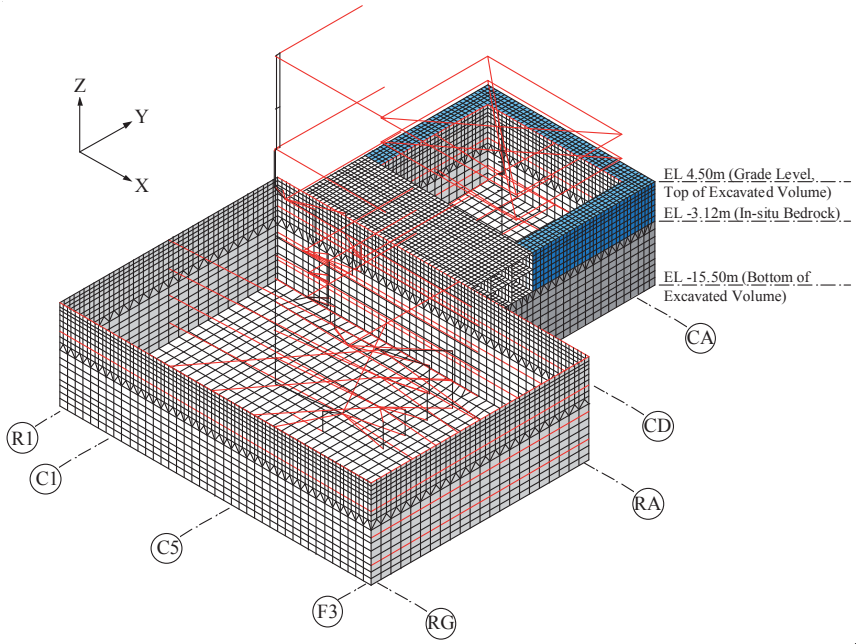

(a) Fully Embedded (FE) Model

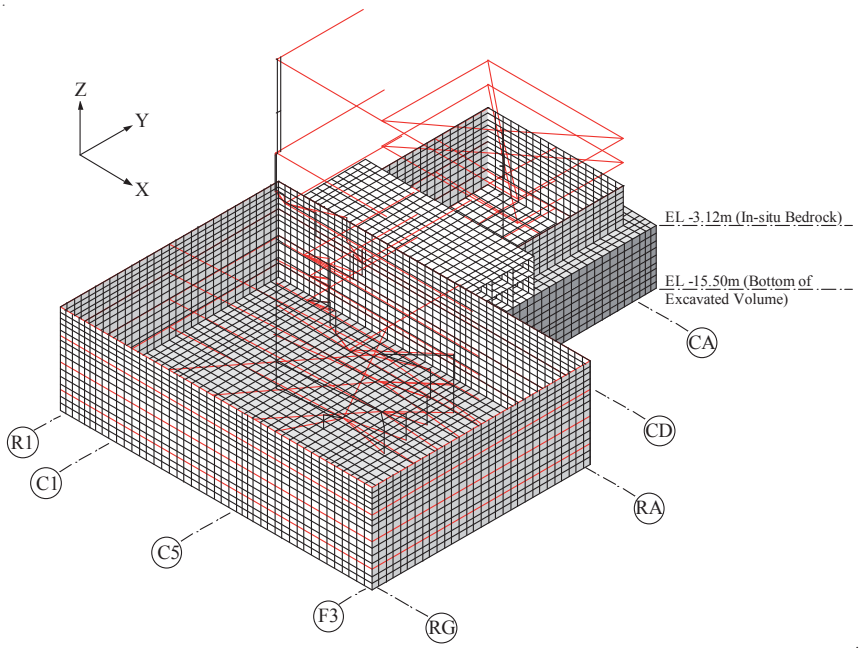

(b) Partially Embedded (PE) Model

Figure 4.3-1 Overview of CB-RB/FB SASSI Model

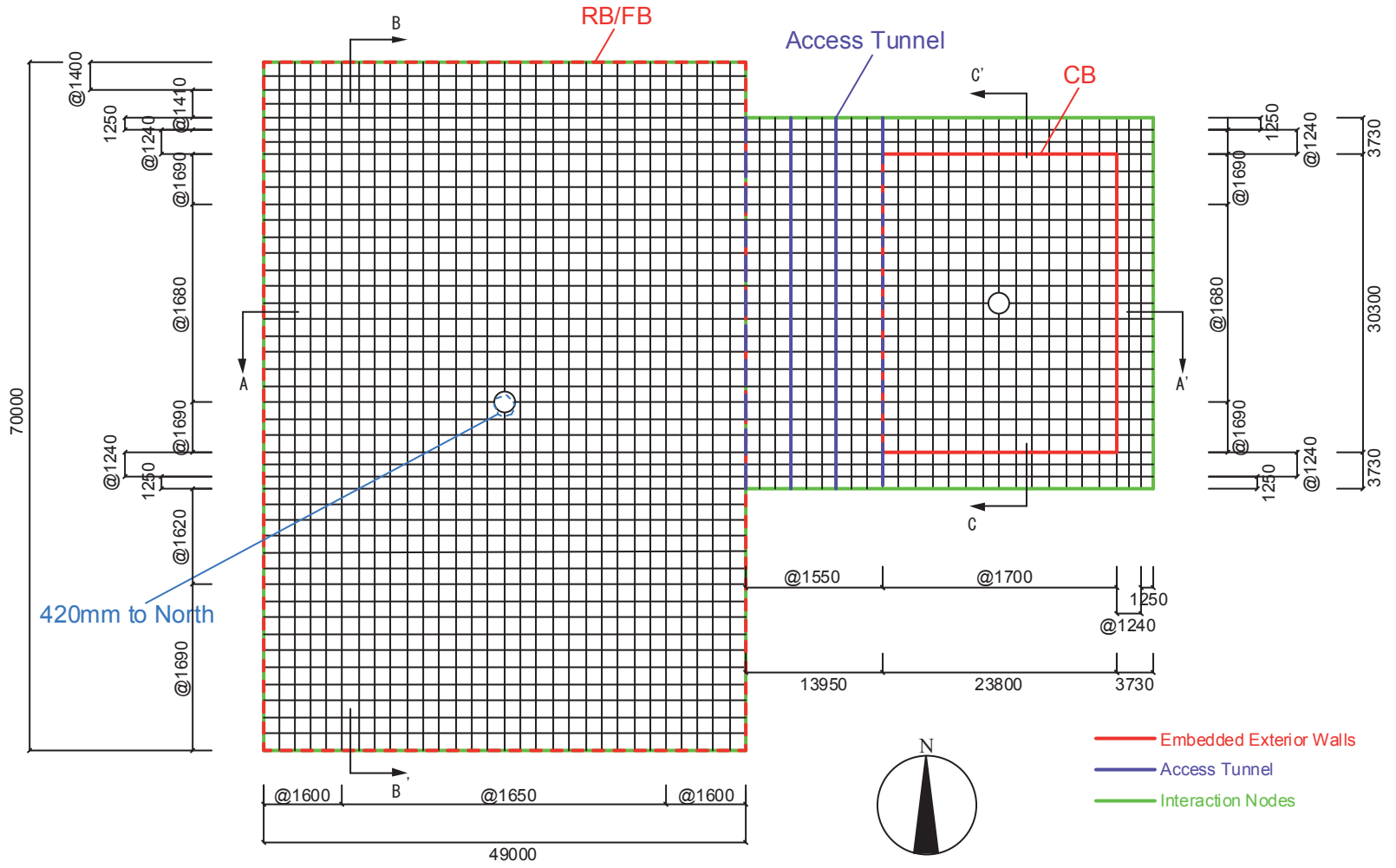

Figure 4.3-2 Plan View of CB-RB/FB SASSI Model (Partially Embedded model shown as example)

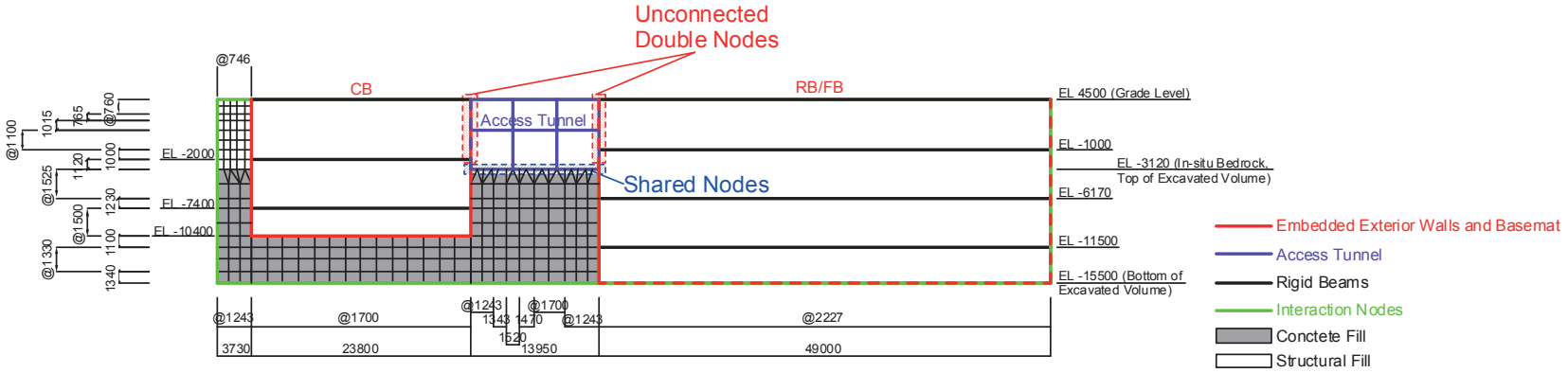

Note: The meshing of exterior walls shall be consistent with the excavated volume model

Figure 4.3-3(a) Section A-A' Structure Model (FE)

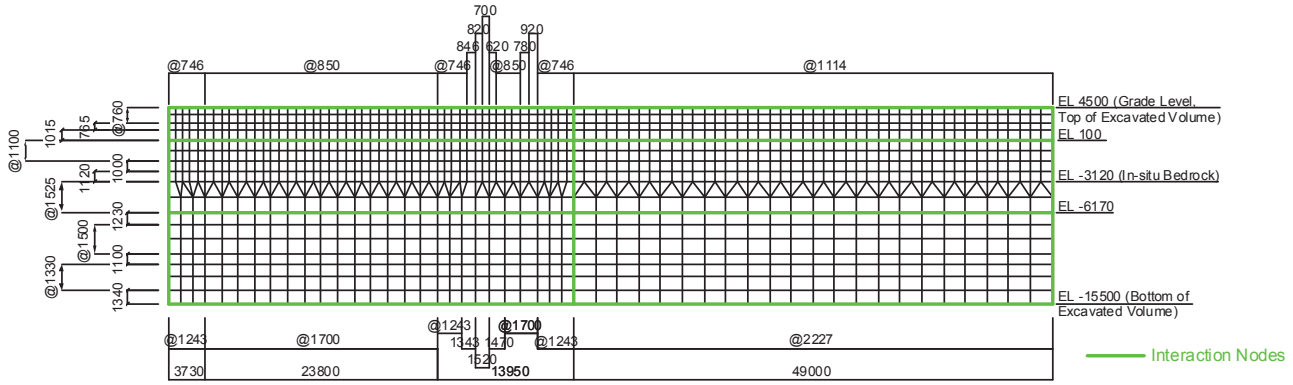

Figure 4.3-3(b) Section A-A' Excavated Volume Model (FE)

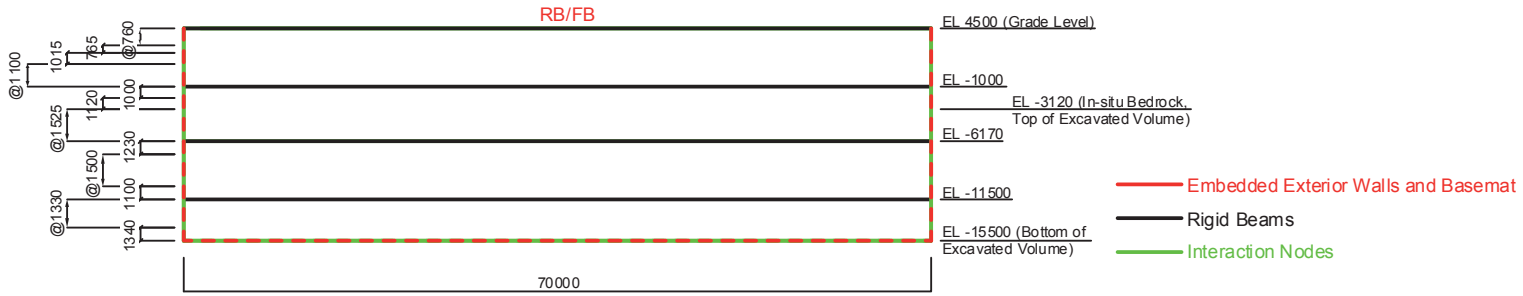

Note: The meshing of exterior walls shall be consistent with the excavated volume model

Figure 4.3-3(c) Elevation B-B' Structure Model (FE)

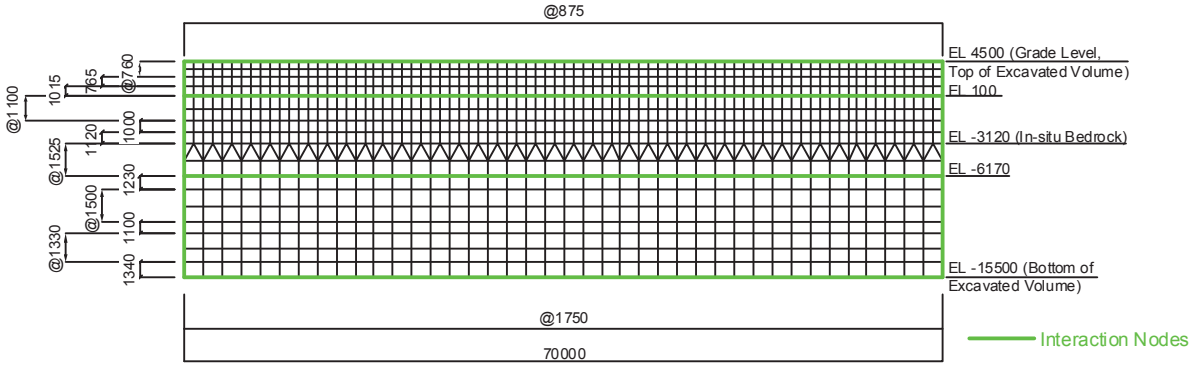

Figure 4.3-3(d) Elevation B-B' Excavated Volume Model (FE)

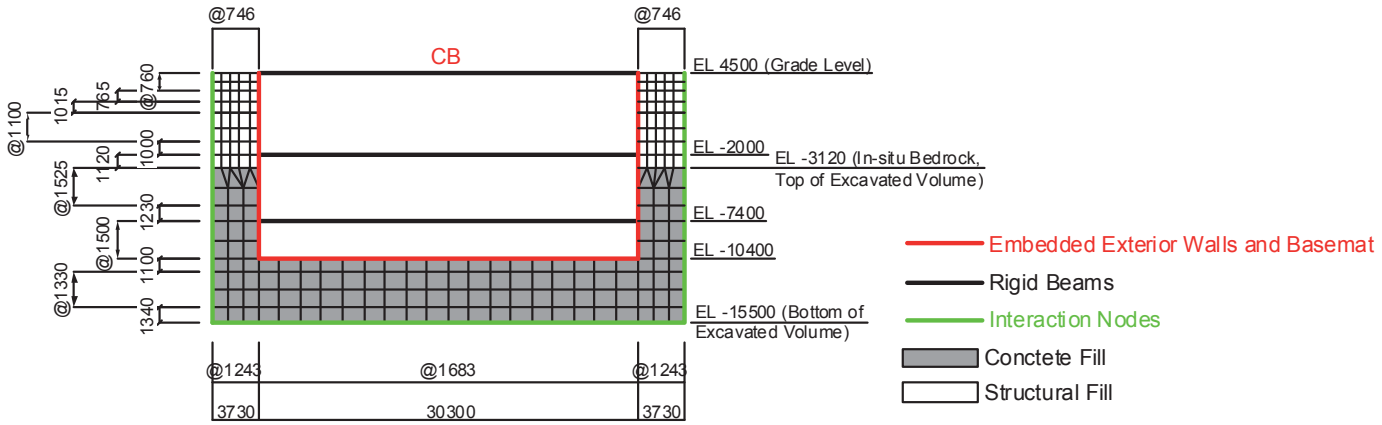

Note: The meshing of exterior walls shall be consistent with the excavated volume model

Figure 4.3-3(e) Elevation C-C' Structure Model (FE)

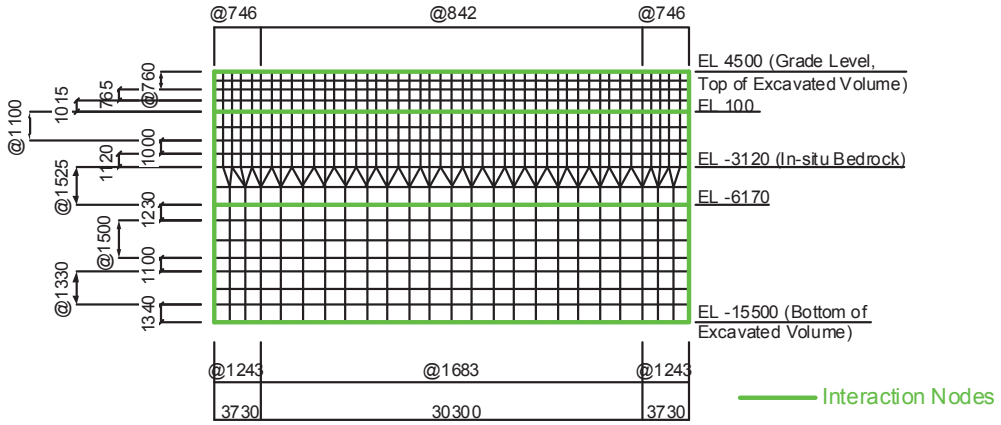

Figure 4.3-3(f) Elevation C-C' Excavated Volume Model (FE)

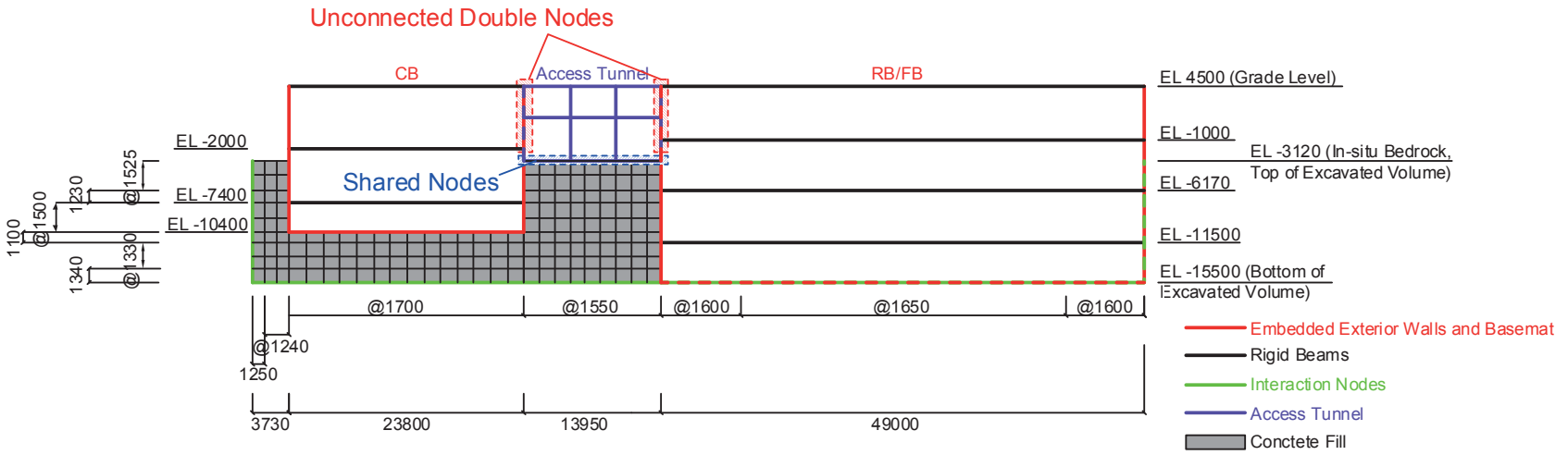

Note: The meshing of exterior walls shall be consistent with the structural model used for UB soil profiles.

Figure 4.3-4(a) Section A-A' Structure Model (PE)

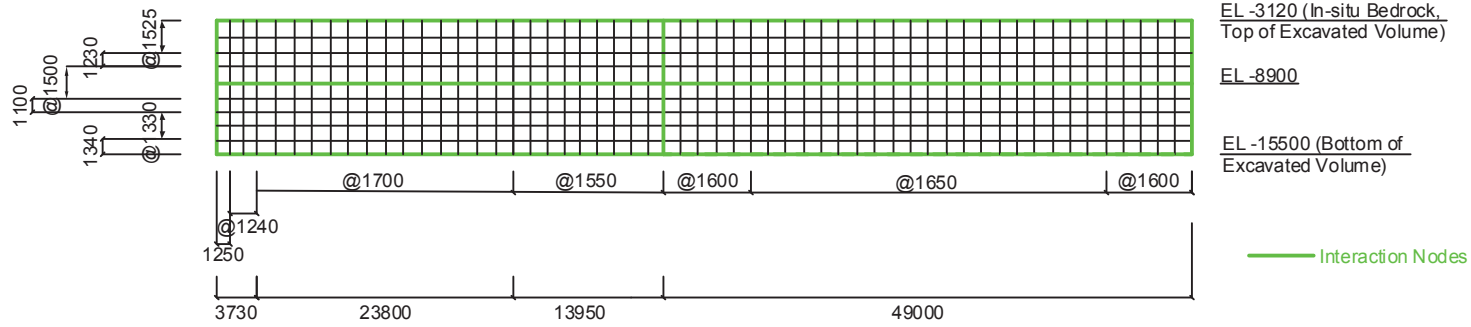

Figure 4.3-4(b) Section A-A' Excavated Volume Model (PE)

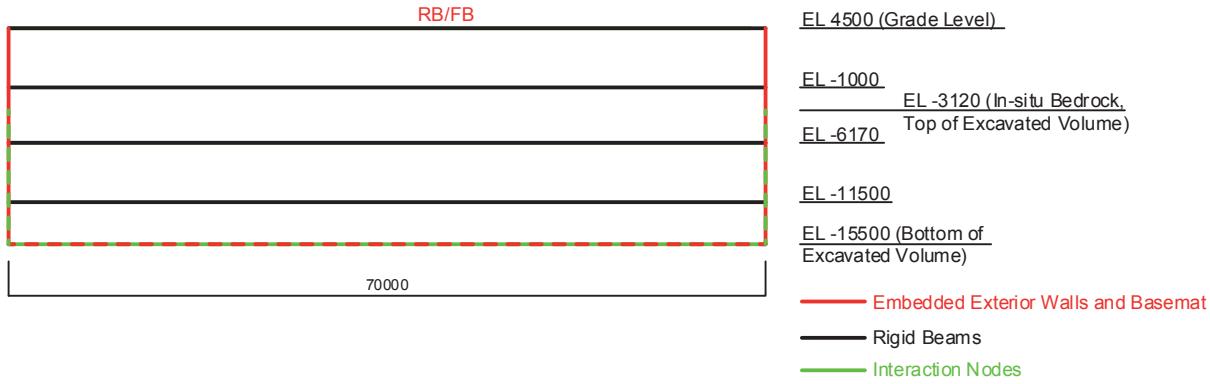

Note: The meshing of exterior walls shall be consistent with the structural model used for UB soil profiles.

Figure 4.3-4(c) Elevation B-B' Structure Model (PE)

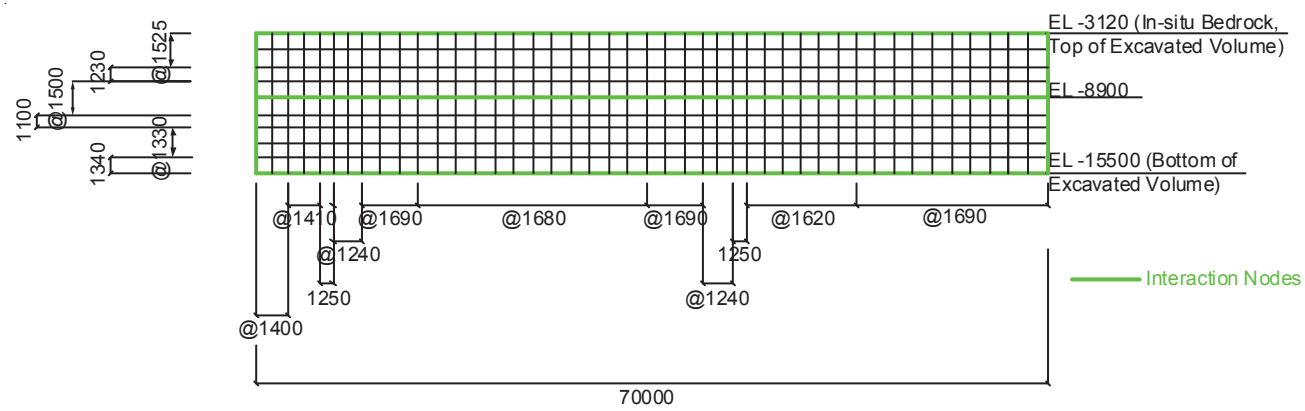

Figure 4.3-4(d) Elevation B-B' Excavated Volume Model (PE)

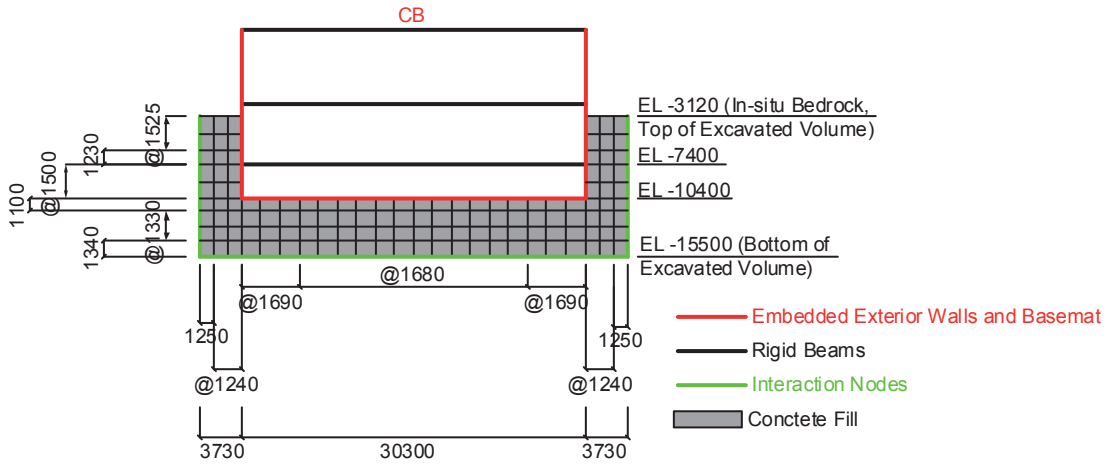

Note: The meshing of exterior walls shall be consistent with the structural model used for UB soil profiles.

Figure 4.3-4(e) Elevation C-C' Structure Model (PE)

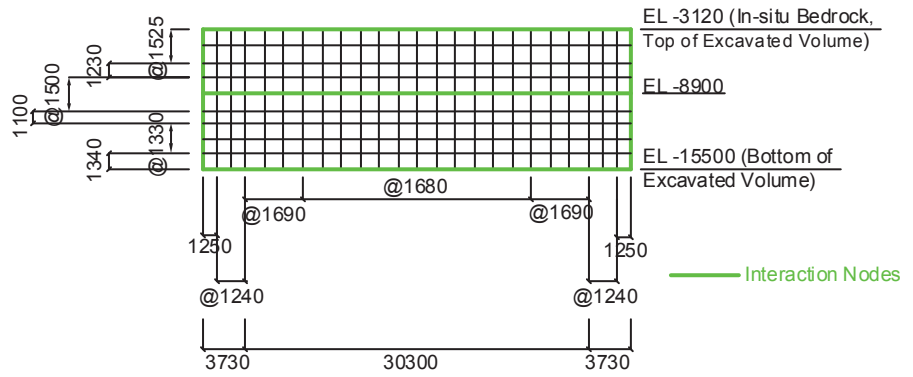

Figure 4.3-4(f) Elevation C-C' Excavated Volume Model (PE)

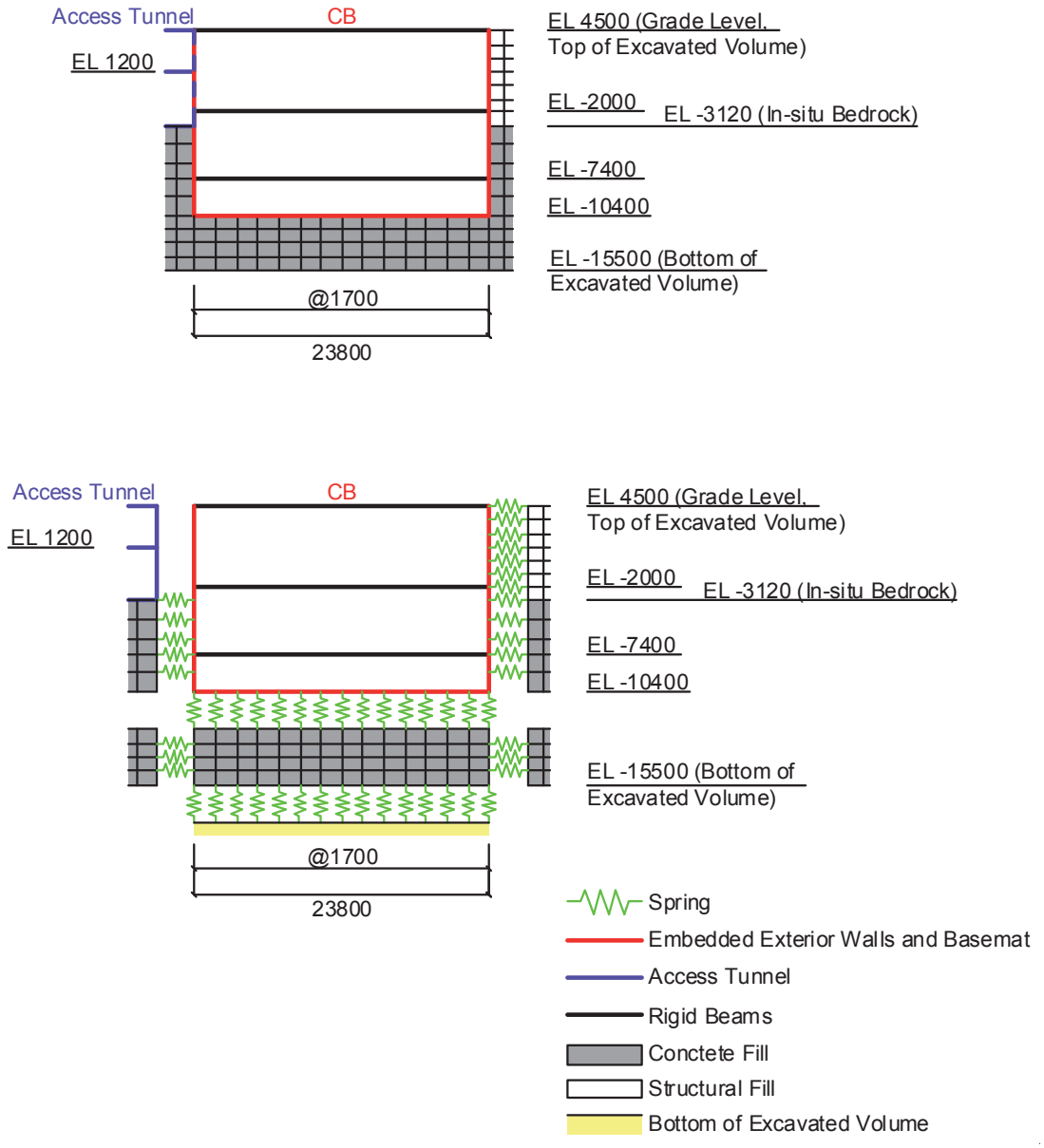

Figure 4.3-5 Locations of Spring Elements for CB Exterior Wall/Backfill Interfaces

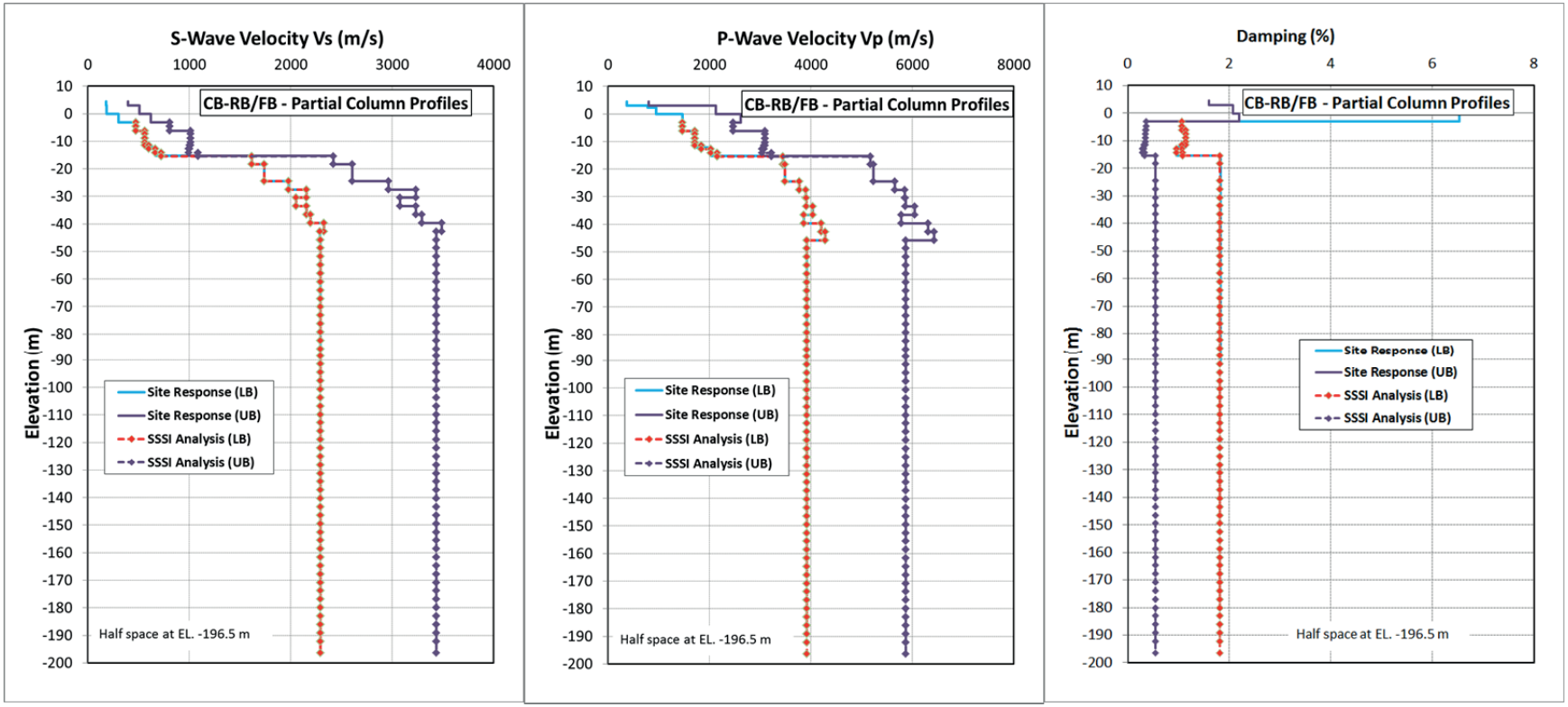

Figure 4.3-6 CB-RB/FB Combined Model Input Partial Column Subgrade Profiles

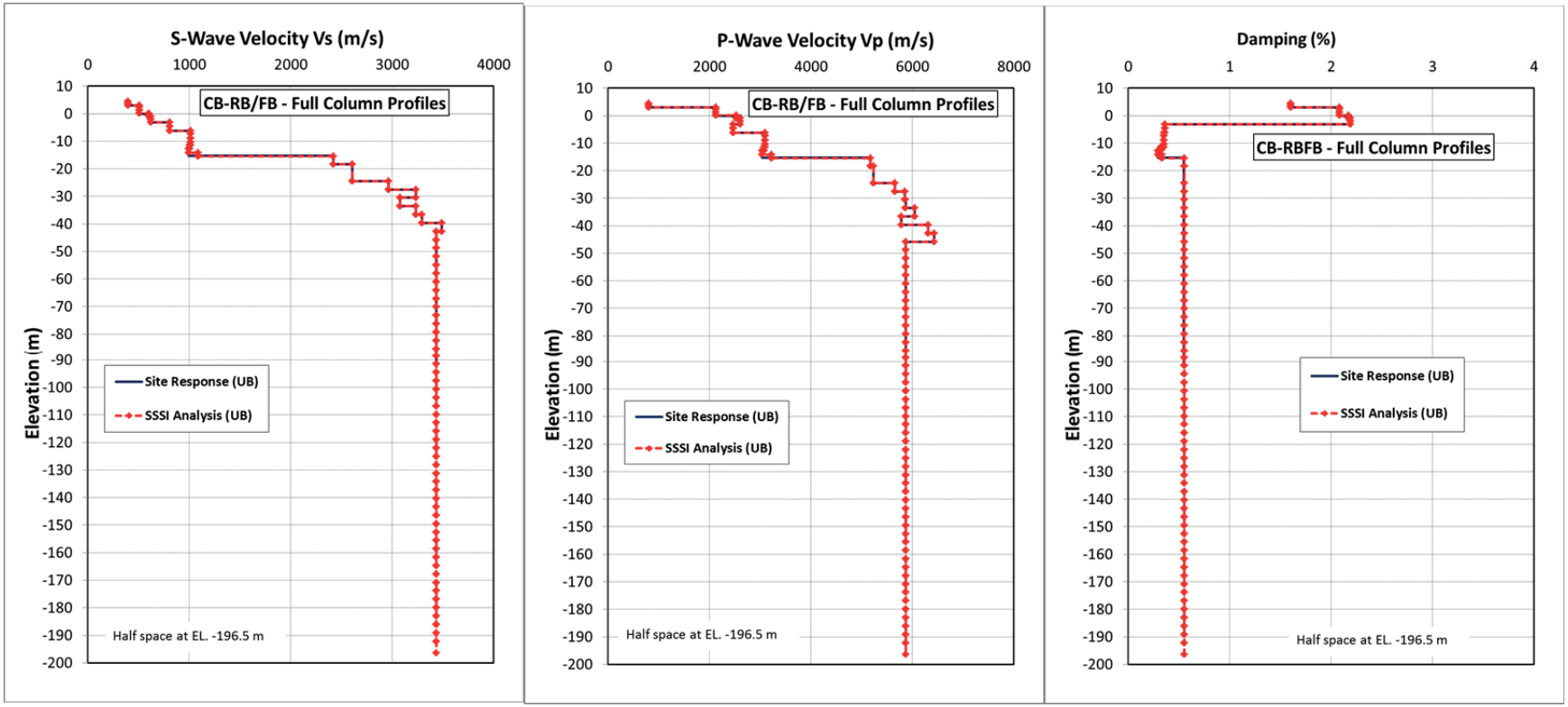

Figure 4.3-7 CB-RB/FB Combined Model Input Full Column Subgrade Profiles

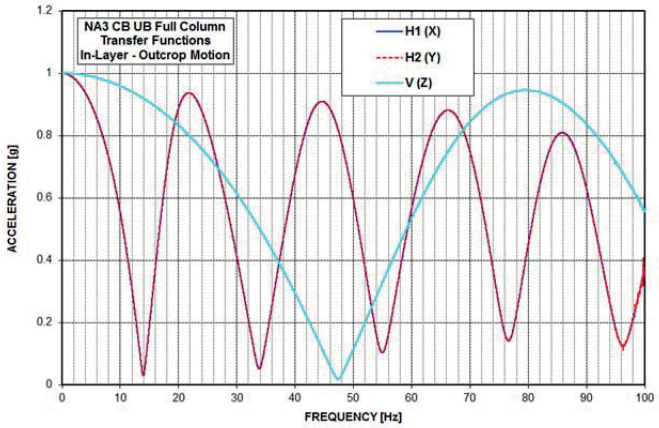

(a) UB Full Column Profile

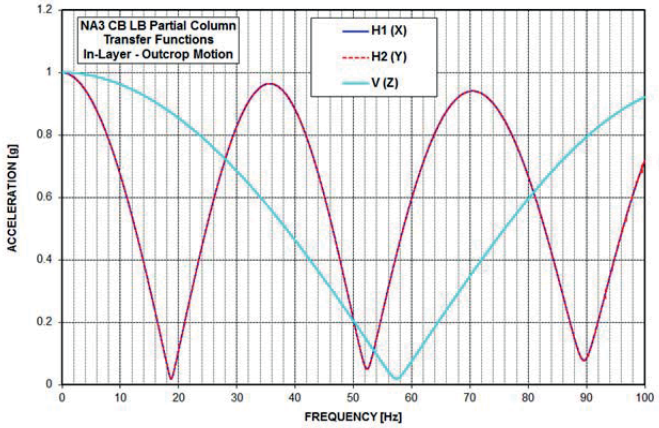

(b) LB Partial Column Profile

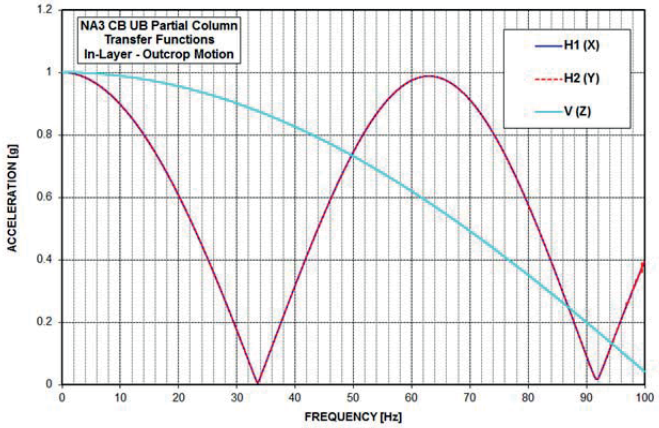

(c) UB Partial Column Profile

Figure 5.1-1 Transfer Functions for Transformation of CB In-Layer Motion into Outcrop Motion

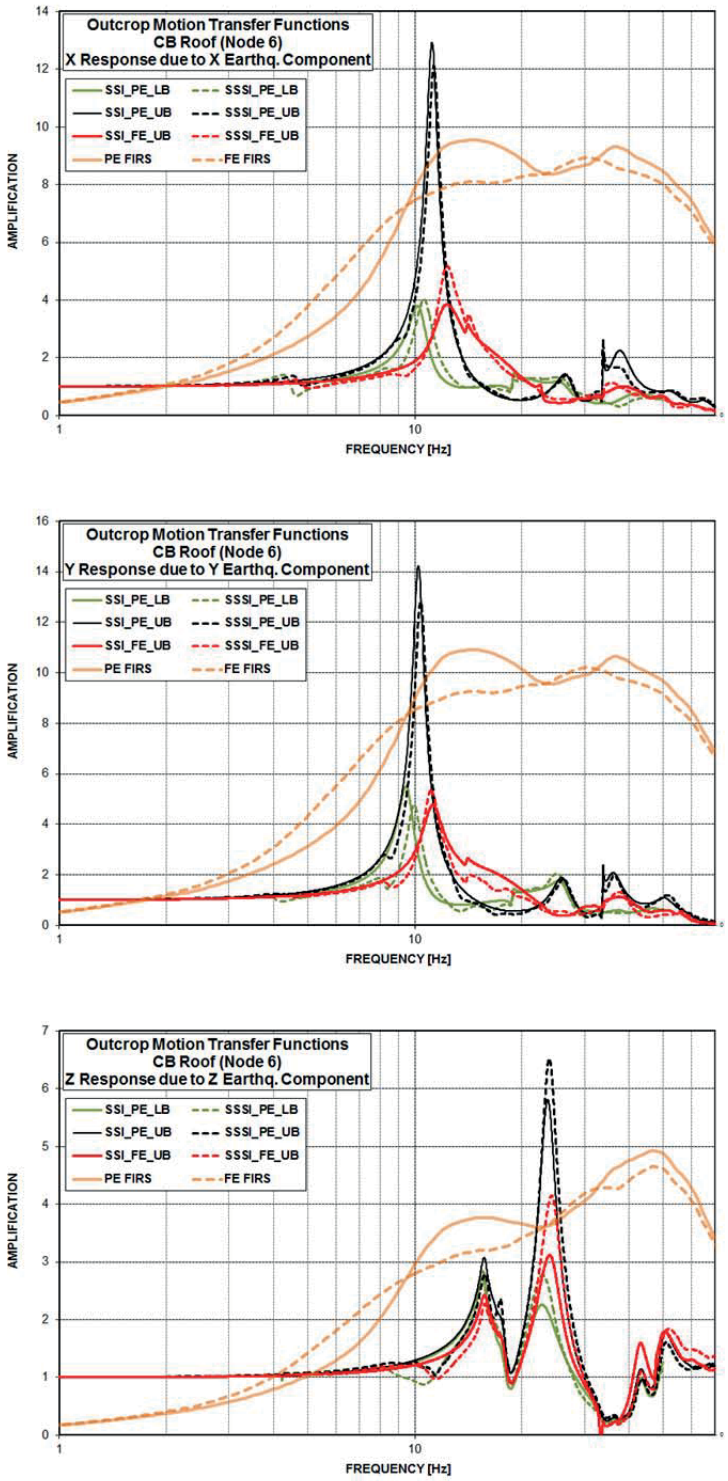

Figure 5.1-2 Comparison of Outcrop Transfer Functions for Co-Directional Response of CB Top

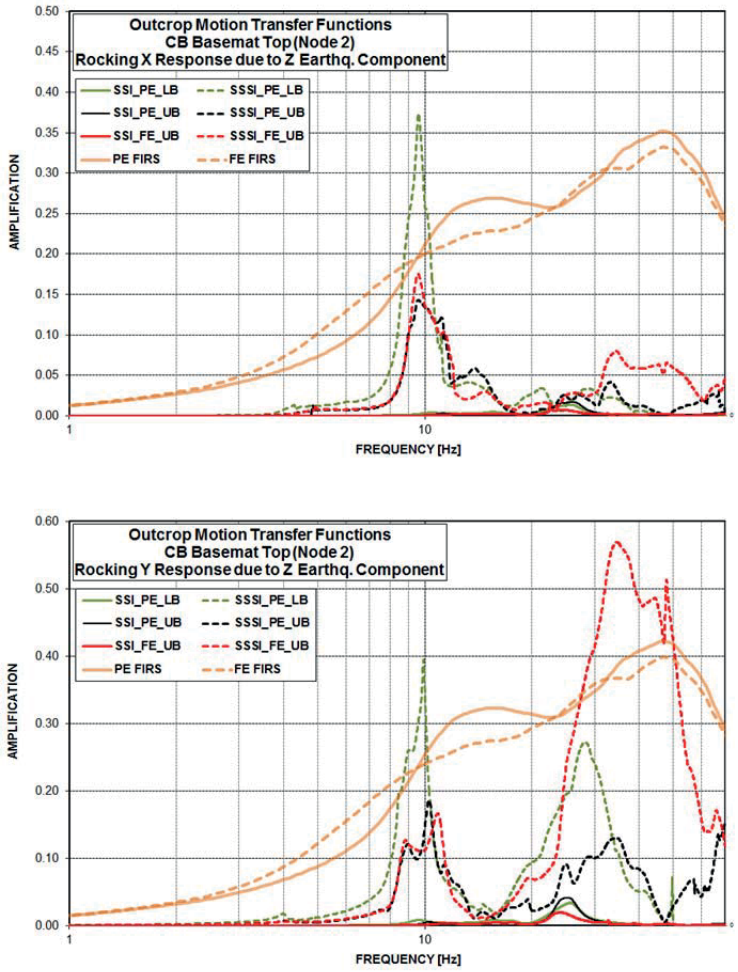

Figure 5.1-3 Comparison of Rotational Outcrop Transfer Functions for Response of CB Basemat

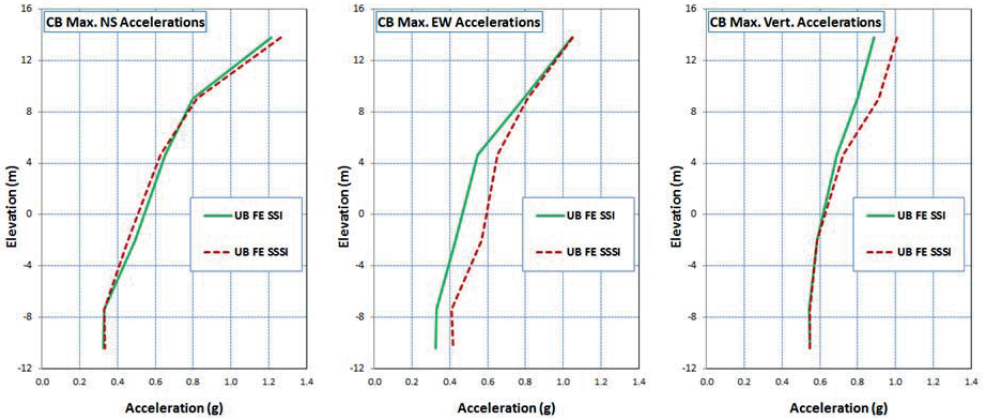

(a) UB Full Column Profile

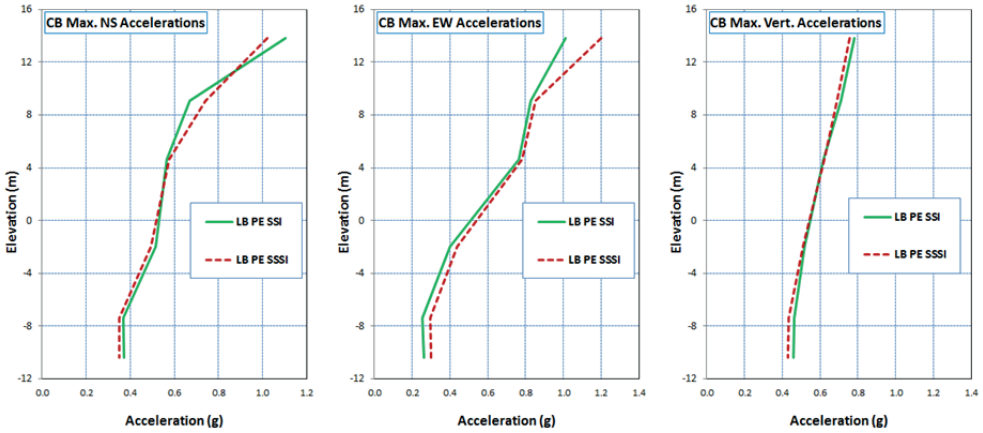

(b) LB Partial Column Profile

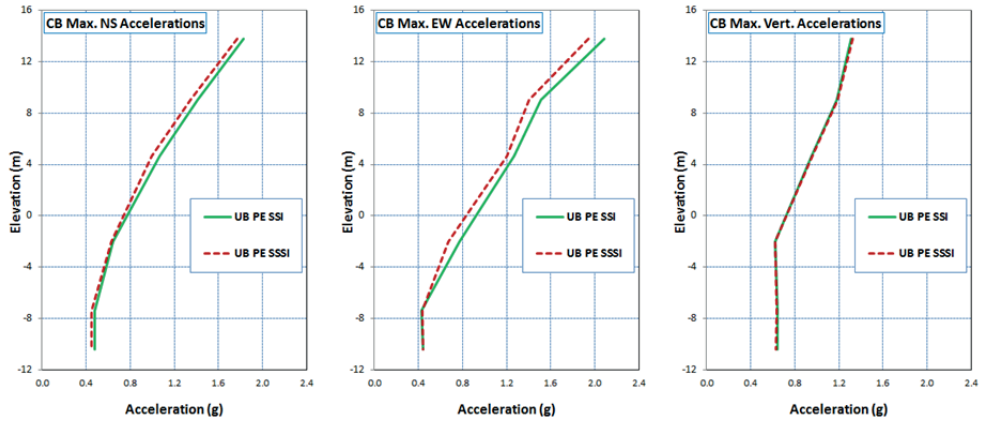

(c) UB Partial Column Profile

Figure 5.2-1 Comparison of CB Maximum Accelerations

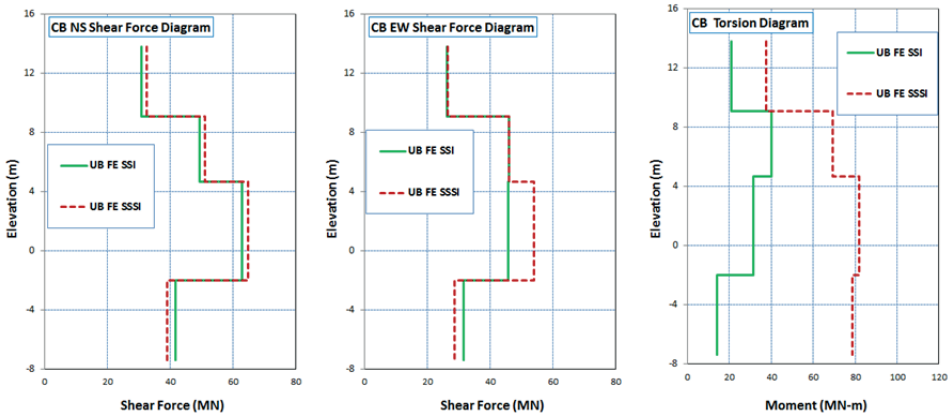

(a) UB Full Column Profile

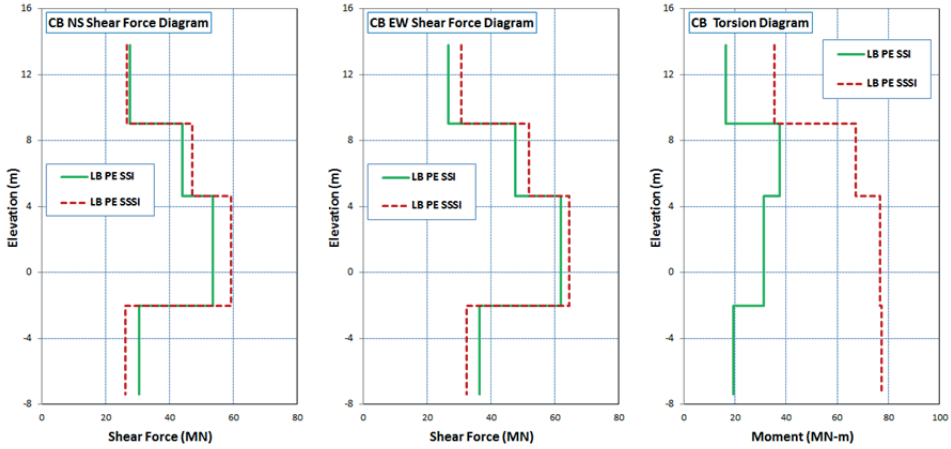

(b) LB Partial Column Profile

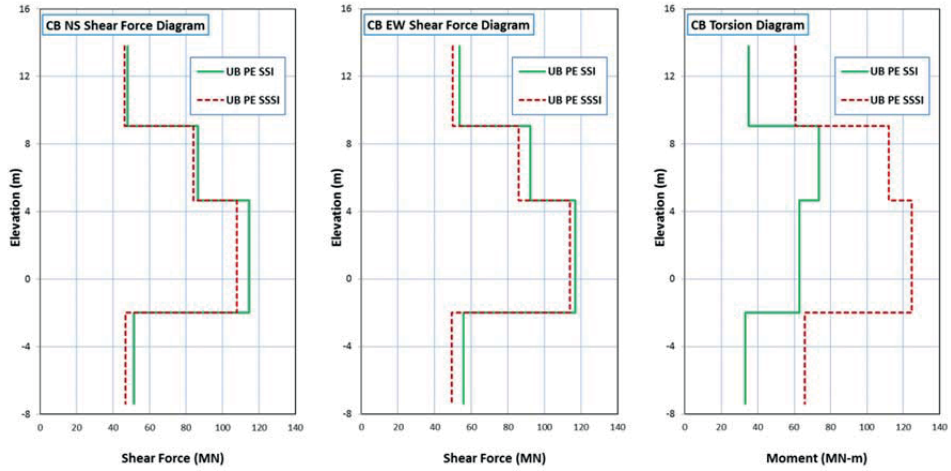

(c) UB Partial Column Profile

Figure 5.2-2 Comparison of CB Maximum Shear Forces and Torsion

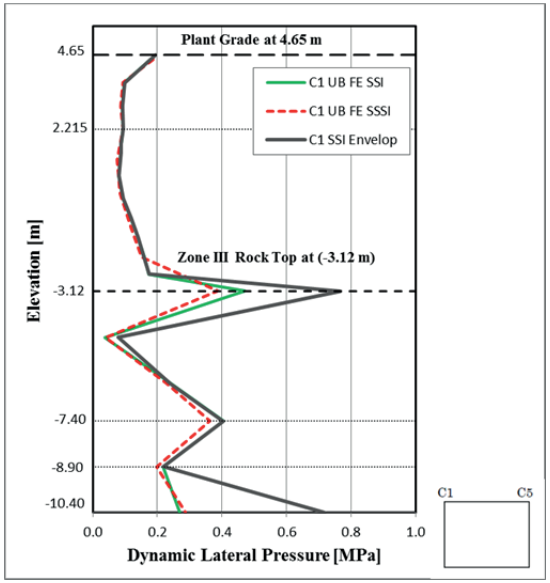

(a) UB Full Column Profiles

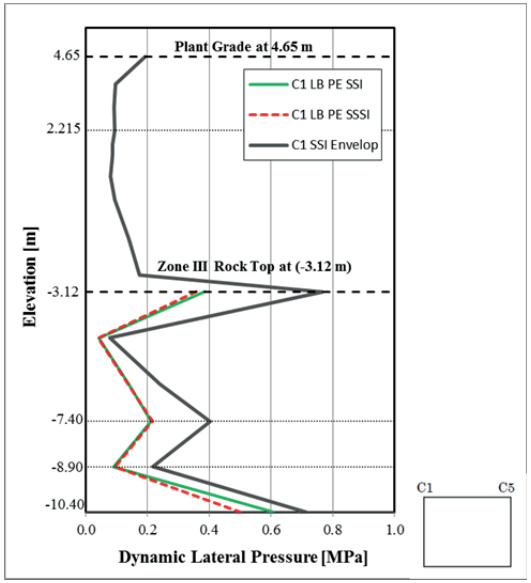

(b) LB Partial Column Profiles

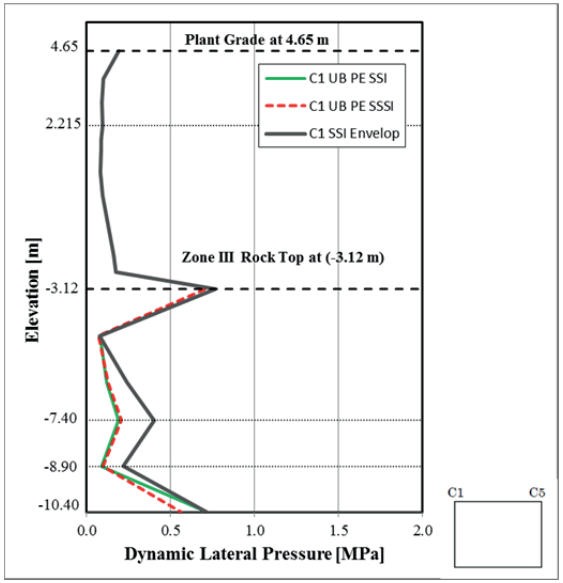

(c) UB Partial Column Profiles

Figure 5.3-1 Comparison of Dynamic Lateral Pressures CB Below-Grade Walls at Column Line C1

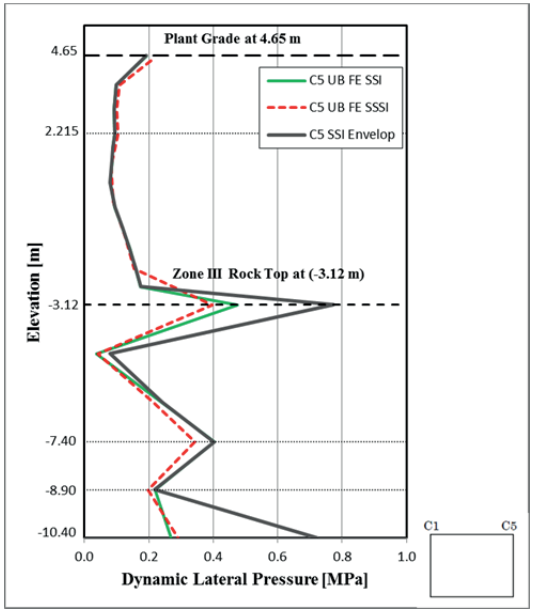

(a) UB Full Column Profiles

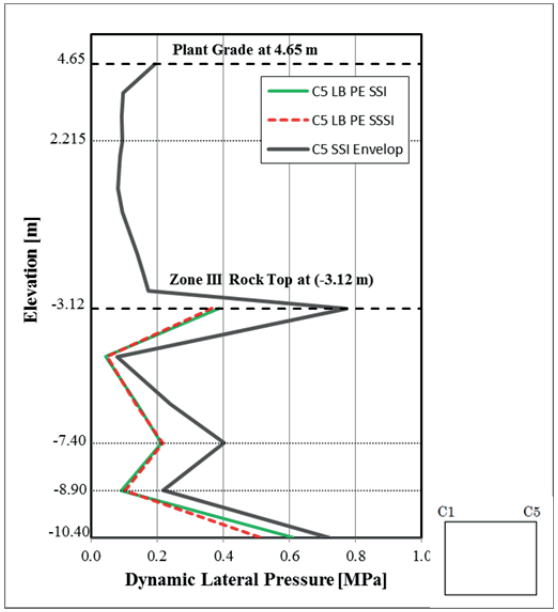

(b) LB Partial Column Profiles

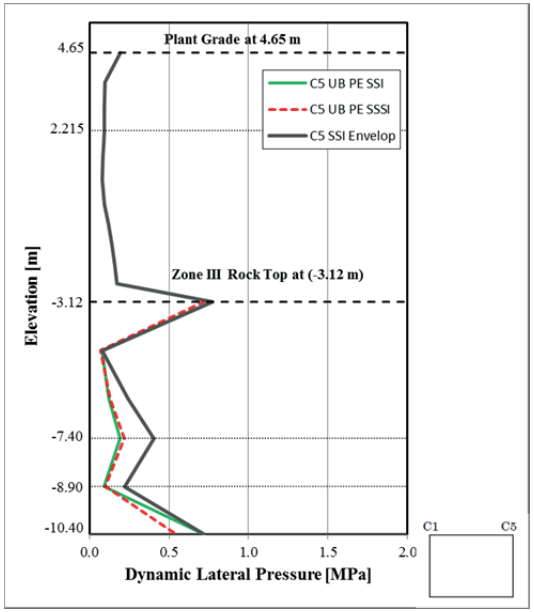

(c) UB Partial Column Profiles

Figure 5.3-2 Comparison of Dynamic Lateral Pressures CB Below-Grade Walls at Column Line C5

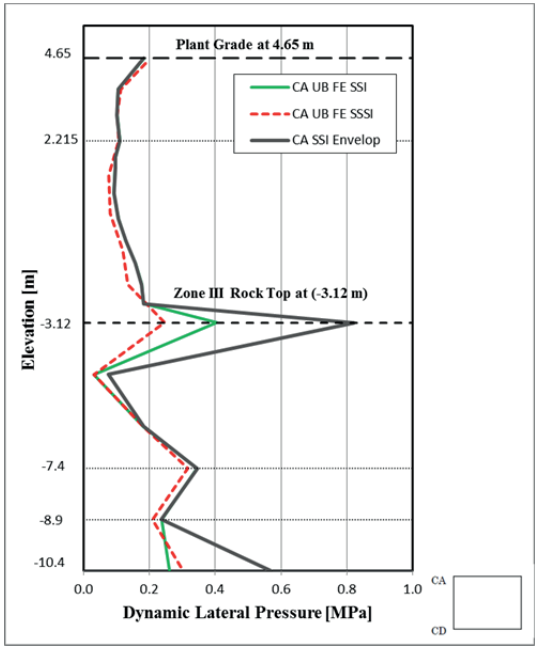

(a) UB Full Column Profiles

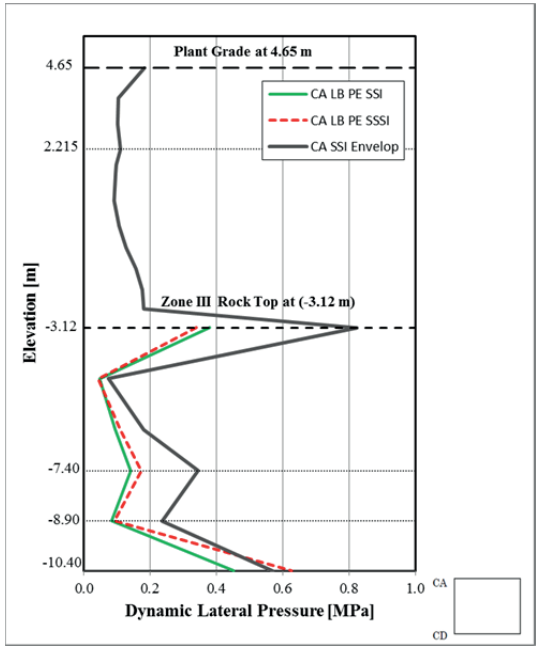

(b) LB Partial Column Profiles

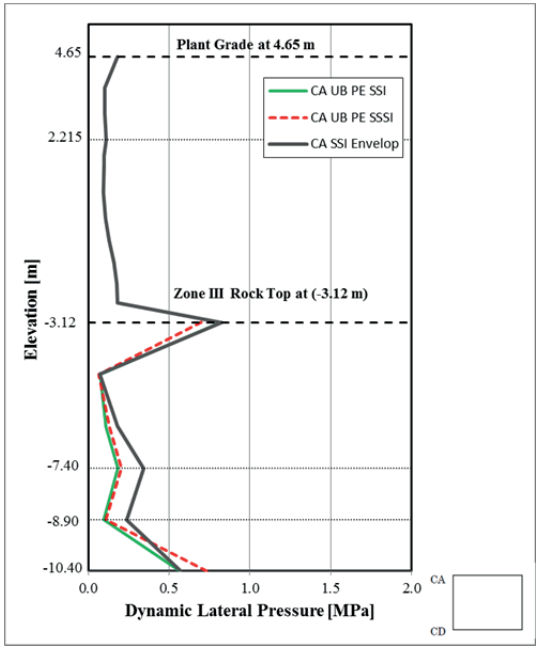

(c) UB Partial Column Profiles

Figure 5.3-3 Comparison of Dynamic Lateral Pressures CB Below-Grade Walls at Column Line CA

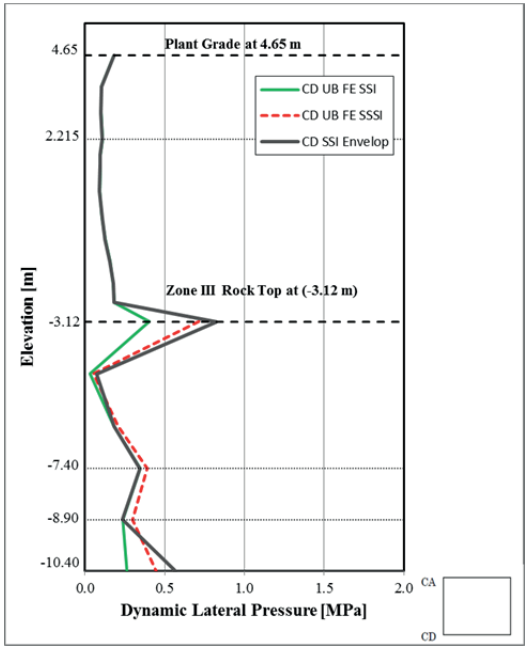

(a) UB Full Column Profiles

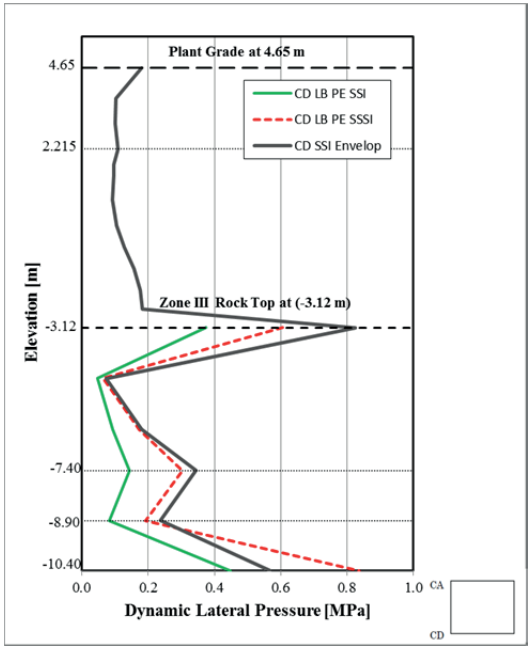

(b) LB Partial Column Profiles

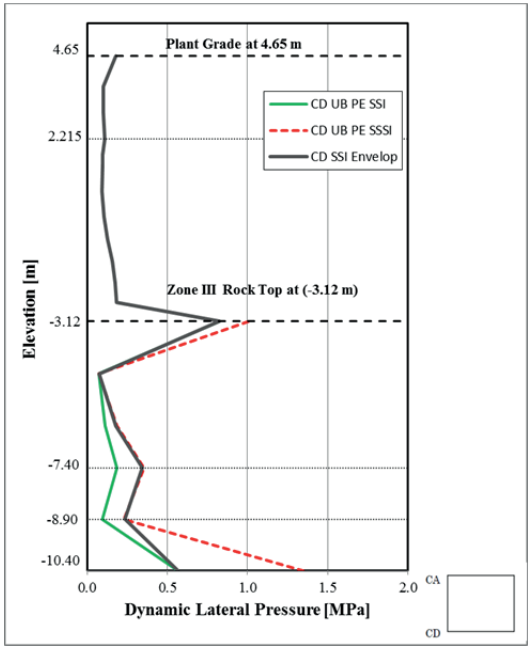

(c) UB Partial Column Profiles

Figure 5.3-4 Comparison of Dynamic Lateral Pressures CB Below-Grade Walls at Column Line CD

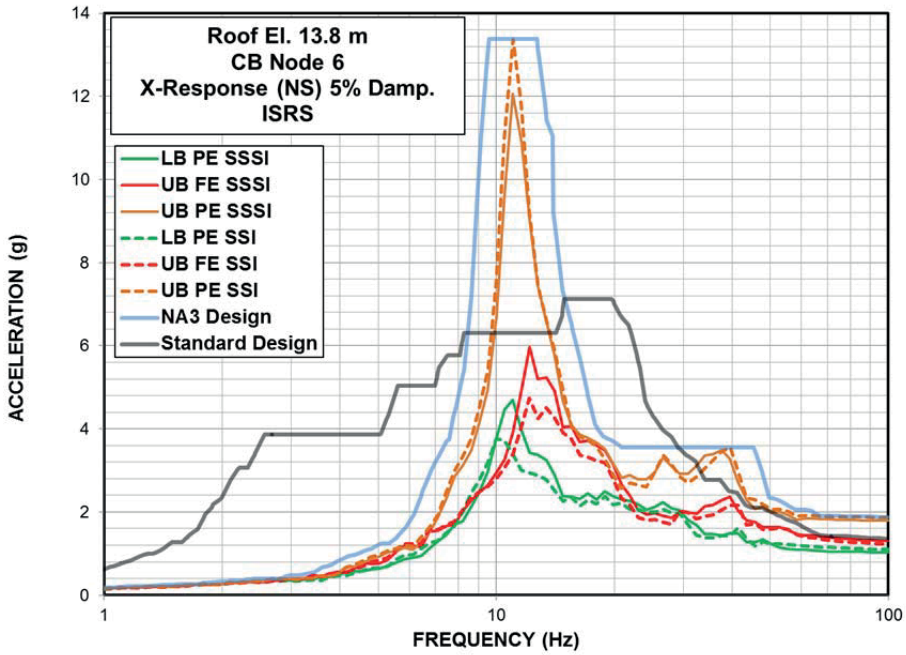

(a) CB Roof at Elevation 13.8 m

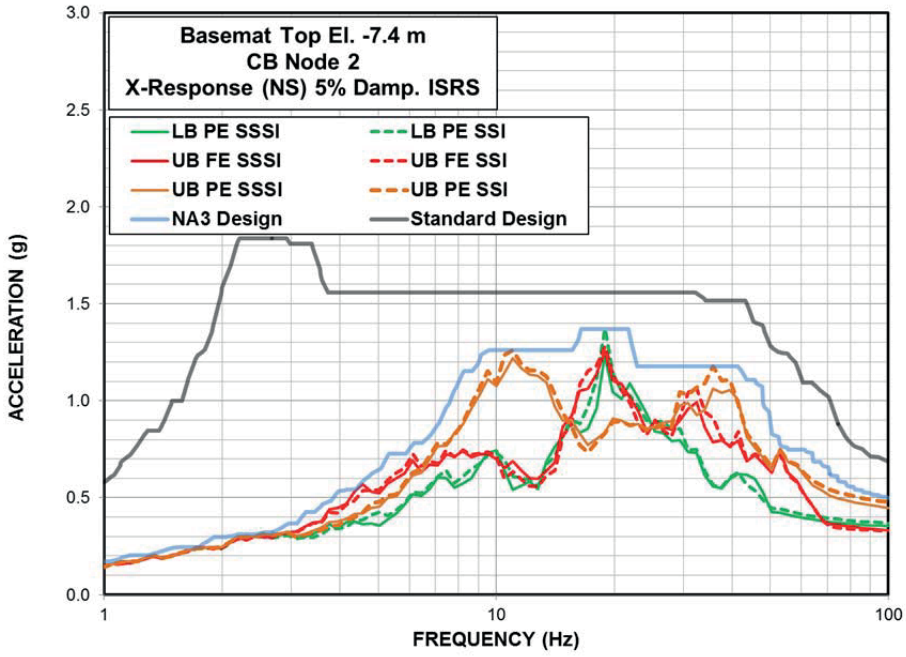

(b) Top of CB Basemat at Elevation - 7.4 m

Figure 5.4-1 Comparison of ISRS for CB Response in NS (X) Direction

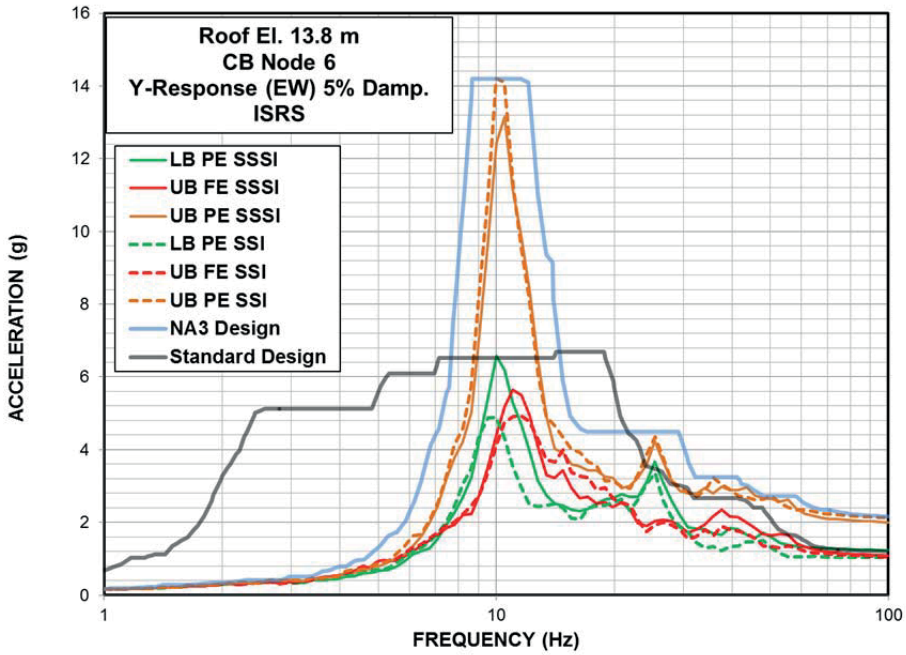

(a) CB Roof at Elevation 13.8 m

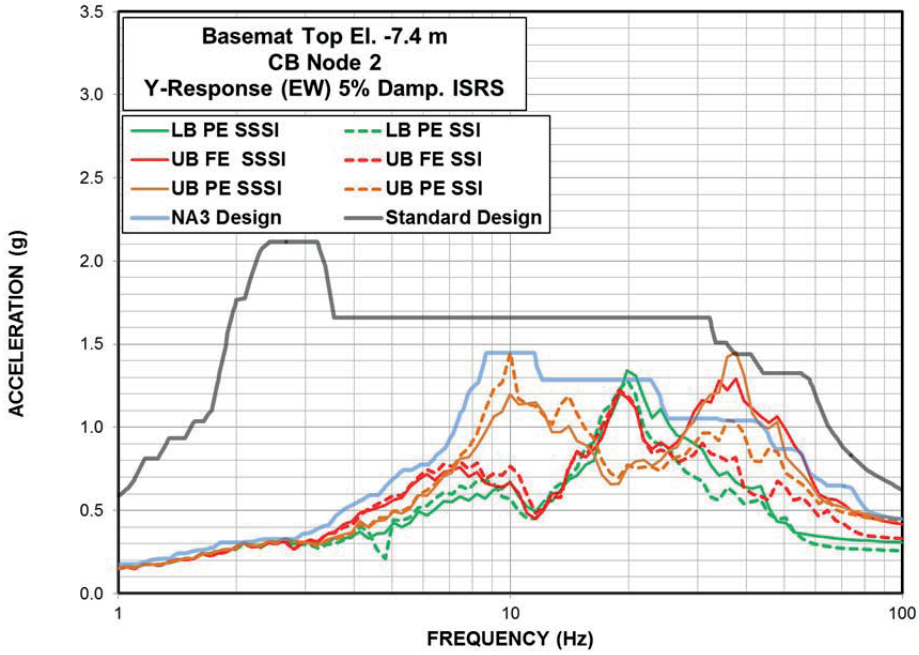

(b) Top of CB Basemat at Elevation - 7.4 m

Figure 5.4-2 Comparison of ISRS for CB Response in EW (Y) Direction

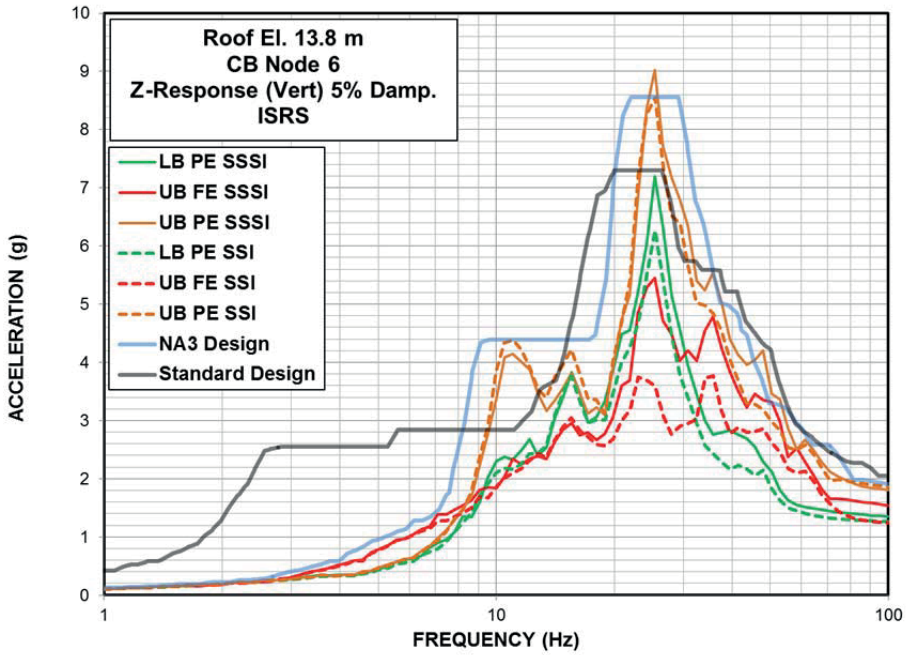

(a) CB Roof at Elevation 13.8 m

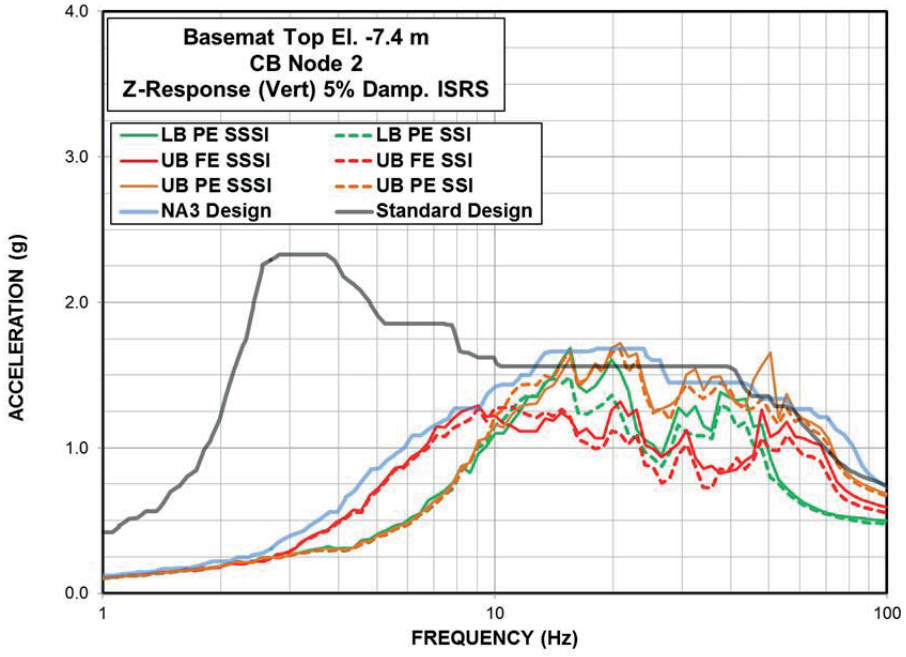

(b) Top of CB Basemat at Elevation - 7.4 m

Figure 5.4-3 Comparison of ISRS for CB Response in Vertical (Z) Direction

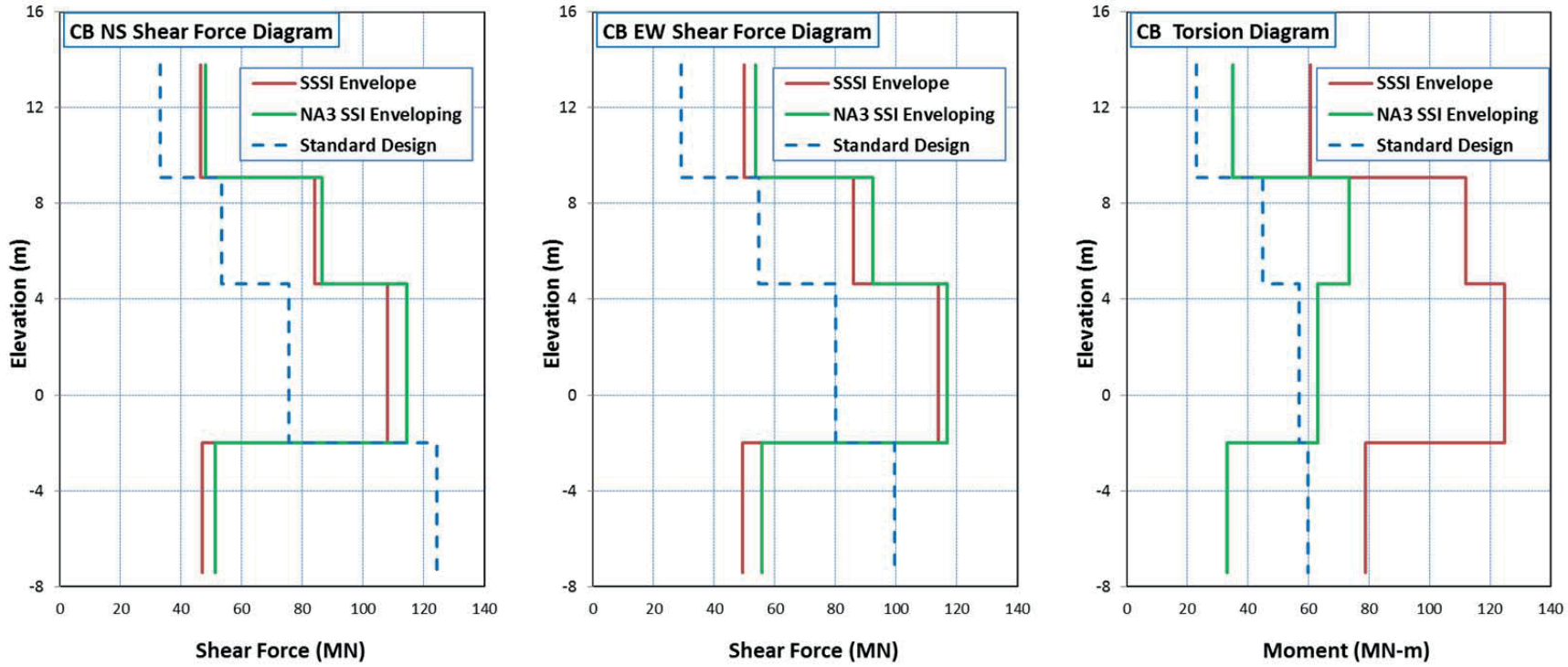

Figure 5.5-1 Comparison of Horizontal Seismic Load Demands on CB Structure

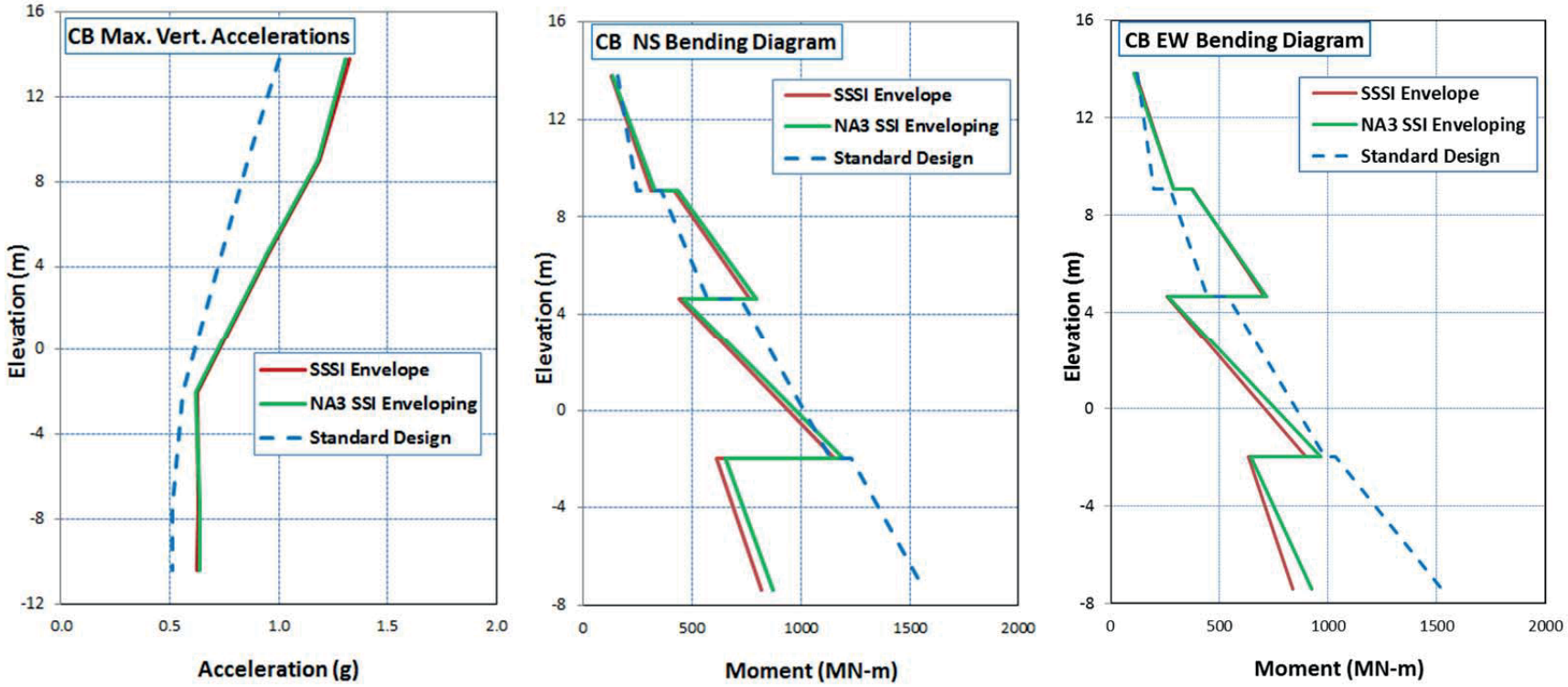

Figure 5.5-2 Comparison of Vertical Seismic Load Demands on CB Structure

APPENDIX A
RESULTS FOR MAXIMUM SEISMIC FORCES AND ACCELERATIONS

LIST OF TABLES

Table A.1 CB Maximum Structural Force and Moment Demands

Elev. (m)	Element No.	Node No.	UB Full Column Profile					LB Partial Column Profile					UB Partial Column Profile				
			Shear (MN)		Bending (MN-m)		Torsion (MN-m)	Shear (MN)		Bending (MN-m)		Torsion (MN-m)	Shear (MN)		Bending (MN-m)		Torsion (MN-m)
			NS	EW	NS	EW		NS	EW	NS	EW		NS	EW	NS	EW	
13.80	1303	6	32.2	26.5	91	86	36.9	26.7	30.7	106	107	35.5	46.4	50.0	129	116	60.8
		5			213	172				212	209				312	291	
9.06	1377	5	51.1	46.0	280	233	68.6	47.0	51.8	294	283	67.1	84.0	85.8	413	380	112.1
		4			482	404				464	462				766	714	
4.65	1302	4	64.6	53.8	225	150	79.6	59.1	64.5	294	196	76.7	108.0	113.9	435	263	124.7
		3			586	421				652	556				1152	908	
-2.00	1301	3	38.8	28.8	180	244	81.7	26.2	32.4	367	382	77.4	46.9	49.3	608	636	65.9
-7.40		2			329	322				482	510				820	846	

Table A.2 CB Maximum Accelerations

Elev. (m)	Node No.	UB Full Column Profile			LB Partial Column Profile			UB Partial Column Profile		
		NS (g)	EW (g)	Vert. (g)	NS (g)	EW (g)	Vert. (g)	NS (g)	EW (g)	Vert. (g)
13.80	6	1.26	1.05	1.01	1.02	1.20	0.76	1.77	1.95	1.33
9.06	5	0.82	0.81	0.91	0.74	0.85	0.69	1.35	1.41	1.19
4.65	4	0.63	0.65	0.72	0.58	0.78	0.62	0.99	1.20	0.96
-2.00	3	0.46	0.57	0.58	0.49	0.44	0.51	0.62	0.67	0.62
-7.40	2	0.33	0.41	0.55	0.35	0.30	0.43	0.45	0.43	0.63
-10.40	1	0.33	0.42	0.55	0.35	0.30	0.43	0.45	0.44	0.63

APPENDIX B
PLOTS OF AMPLITUDES OF ACCELERATION TRANSFER FUNCTIONS FROM SSSI ANALYSES OF CB-RB/FB COMBINED MODEL

LIST OF FIGURES

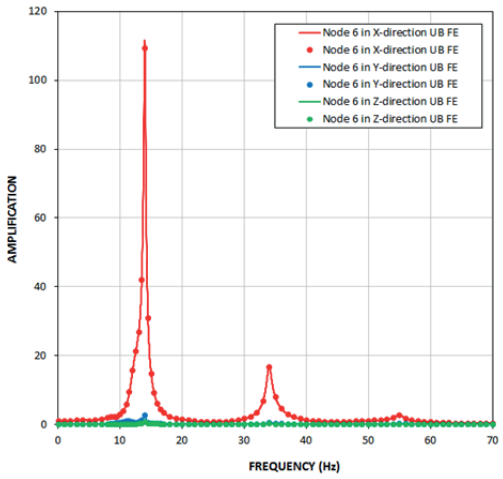

(a)X-Direction Input

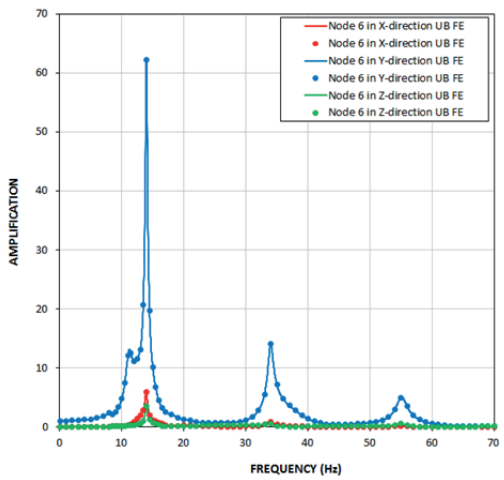

(b) Y-Direction Input

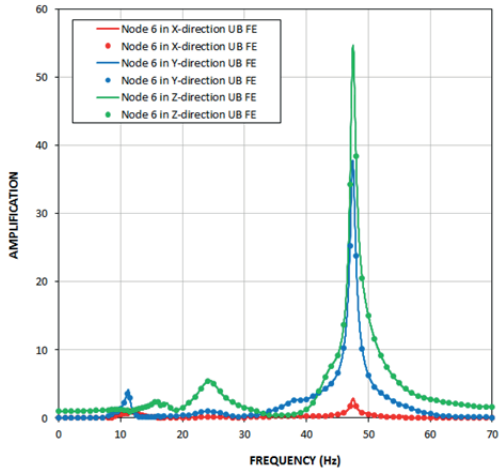

(c) Z-Direction Input

Figure B-1a Transfer Functions of CB Top Response from Analysis of UB Full Column Profile

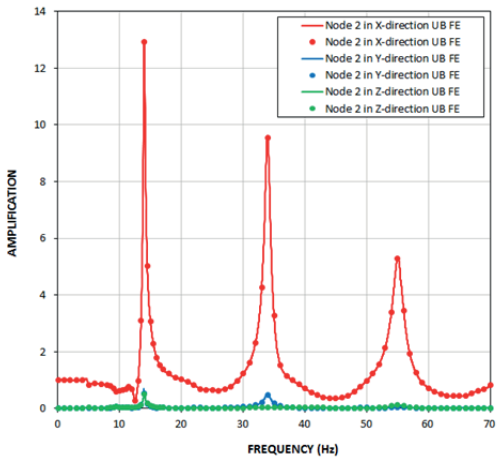

(a)X-Direction Input

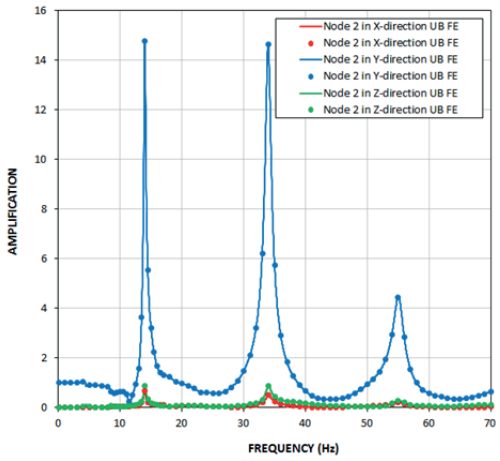

(b) Y-Direction Input

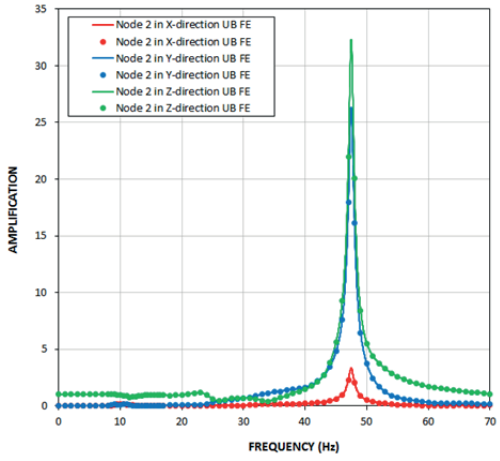

(c) Z-Direction Input

Figure B-1b Transfer Functions of CB Basemat Response from Analysis of UB Full Column Profile

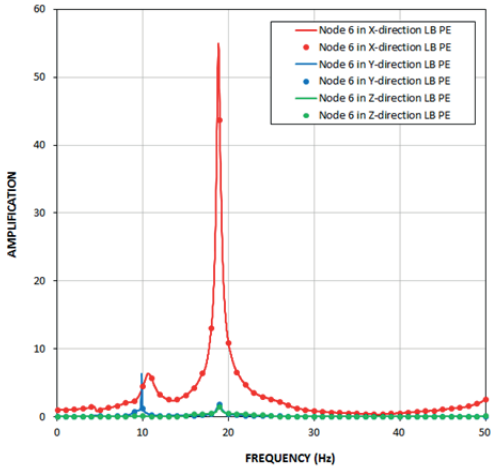

(a)X-Direction Input

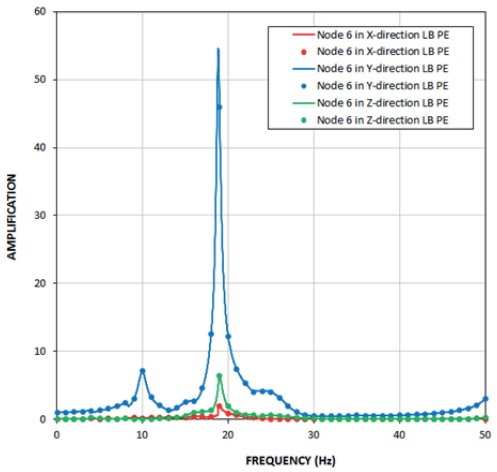

(b) Y-Direction Input

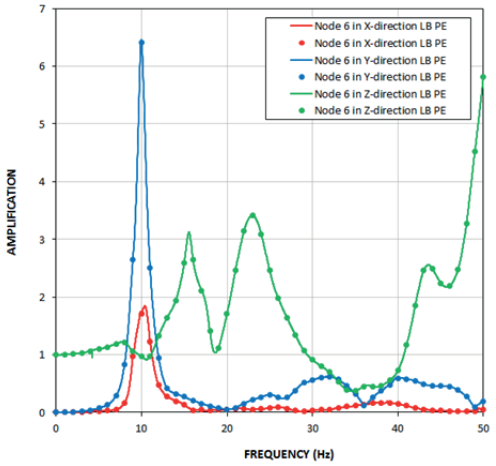

(c) Z-Direction Input

Figure B-2a Transfer Functions of CB Top Response from Analysis of LB Partial Column Profile

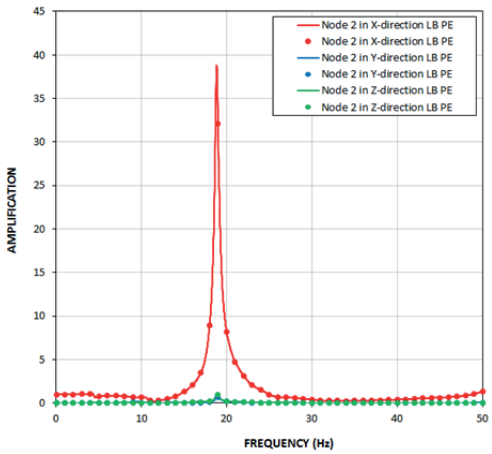

(a)X-Direction Input

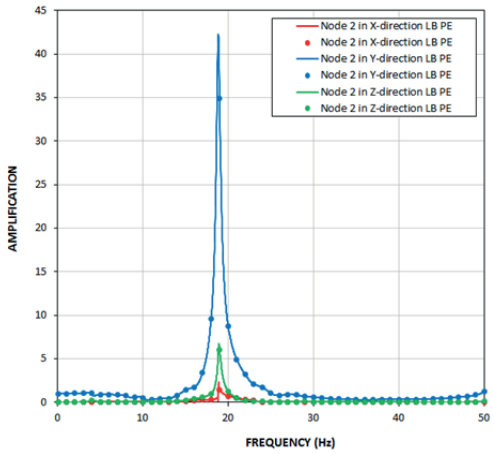

(b) Y-Direction Input

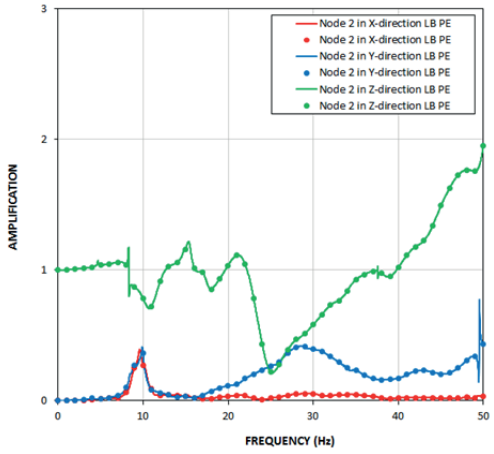

(c) Z-Direction Input

Figure B-2b Transfer Functions of CB Basemat Response from Analysis of LB Partial Column Profile

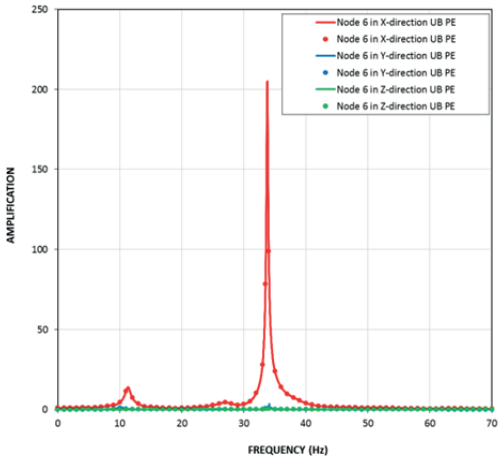

(a)X-Direction Input

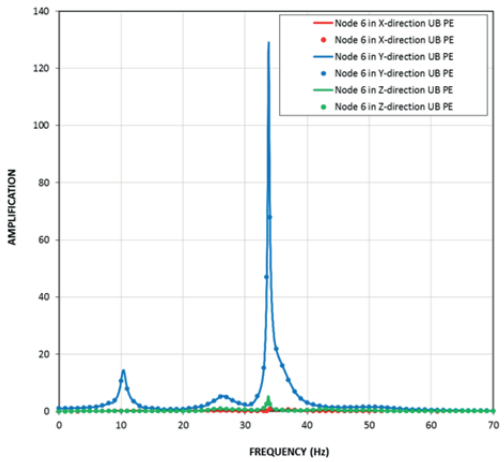

(b) Y-Direction Input

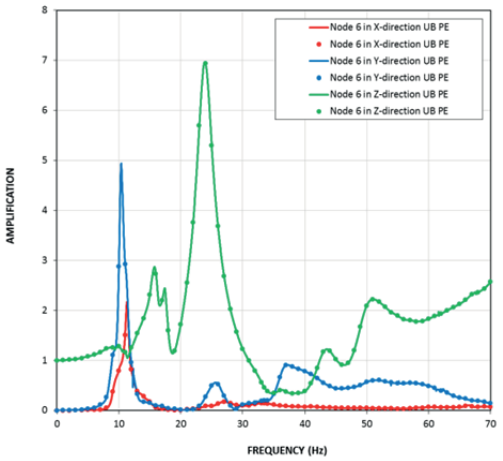

(c) Z-Direction Input

Figure B-3a Transfer Functions of CB Top Response from Analysis of UB Partial Column Profile

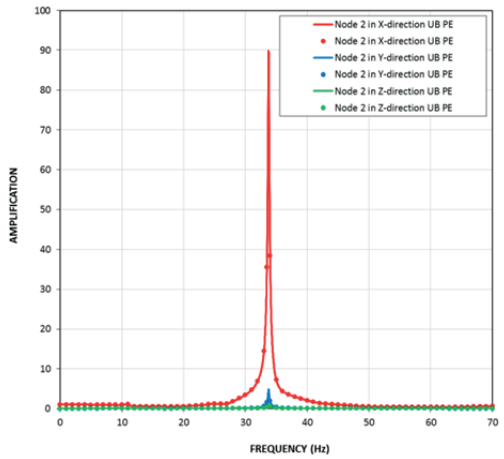

(a)X-Direction Input

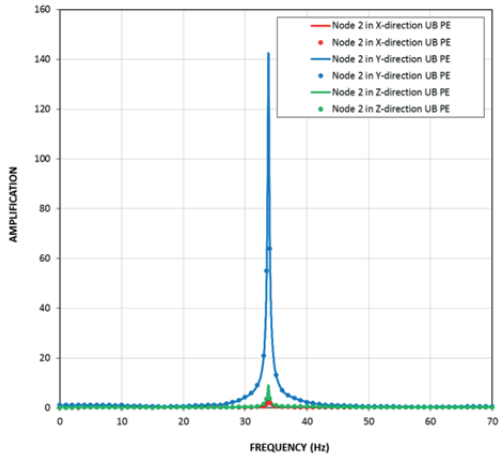

(b) Y-Direction Input

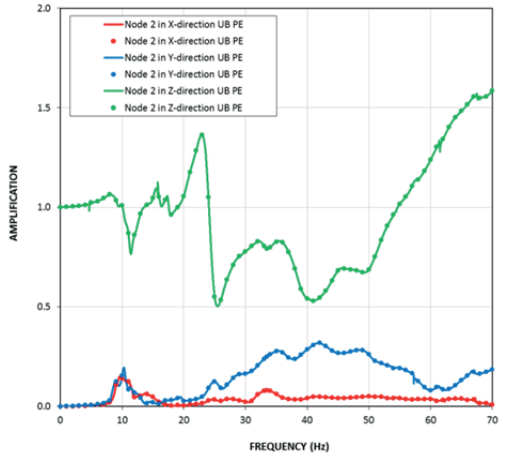

(c) Z-Direction Input

Figure B-3b Transfer Functions of CB Basemat Response from Analysis of UB Partial Column Profile